

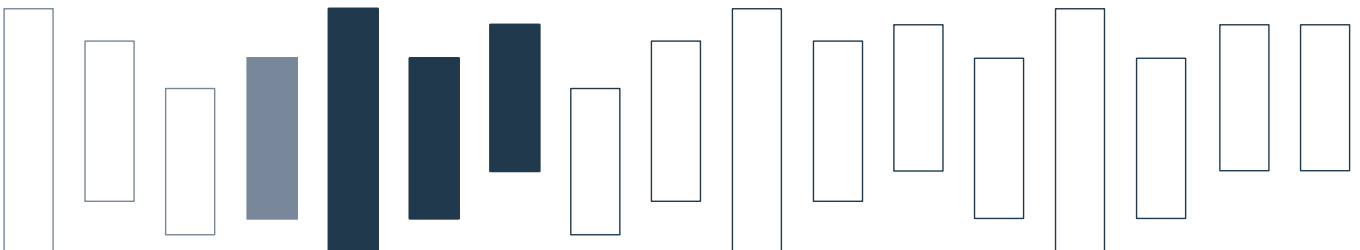


Technical Report AC-TR-21-014

December 2021

Smart Charging of Electric Vehicles Considering SOC-Dependent Maximum Charging Powers

Benjamin Schaden, Thomas Jatschka,
Steffen Limmer, and GÄijnther R. Raidl



This is the authors' copy of a paper that appeared in *MDPI Energies* 14, 22, Article 7755 (December 2021). DOI:

www.ac.tuwien.ac.at/tr

Smart Charging of Electric Vehicles Considering SOC-Dependent Maximum Charging Powers

Benjamin Schaden¹, Thomas Jatschka^{1*}, Steffen Limmer², and Günther R. Raidl¹

¹ Institute of Logic and Computation, TU Wien, Austria; e1527237@student.tuwien.ac.at, {tjatschk|raidl}@ac.tuwien.ac.at

² Honda Research Institute Europe GmbH, 63073 Offenbach, Germany; steffen.limmer@honda-ri.de

* Correspondence: tjatschk@ac.tuwien.ac.at

Abstract: The aim of this work is to schedule the charging of electric vehicles (EVs) at a single charging station such that the temporal availability of each EV as well as the maximum available power at the station are considered. The total costs for charging the vehicles should be minimized w.r.t. time-dependent electricity costs. A particular challenge investigated in this work is that the maximum power at which a vehicle can be charged is dependent on the current state of charge (SOC) of the vehicle. Such a consideration is particularly relevant in the case of fast charging. Considering this aspect for a discretized time horizon is not trivial as the maximum charging power of an EV may also change in between time steps. To deal with this issue, we instead consider the energy by which an EV can be charged within a time step. For this purpose, we show how to derive the maximum charging energy in an exact as well as an approximate way. Moreover, we propose two methods for solving the scheduling problem. The first one is a cutting plane method utilizing a convex hull of the in general nonconcave SOC-power curves. The second method is based on a piecewise linearization of the SOC-energy curve and is effectively solved by branch-and-cut. The proposed approaches are evaluated on benchmark instances, which are partly based on real-world data. To deal with EVs arriving at different times as well as charging costs changing over time, a model based predictive control strategy is usually applied in such cases. Hence, we also experimentally evaluate the performance of our approaches for such a strategy. The results show that optimally solving problems with general piecewise linear maximum power functions requires high computation times. However, problems with concave, piecewise linear maximum charging power functions can efficiently be dealt with by means of linear programming. Approximating an EV's maximum charging power with a concave function may result in practically infeasible solutions, due to vehicles potentially not reaching their specified target SOC. However, our results show that this error is negligible in practice.

Citation: Schaden, B.; Jatschka, T.; Limmer, S.; Raidl, G. Smart Charging of Electric Vehicles Considering SOC-Dependent Maximum Charging Powers. *Energies* **2021**, *1*, 0. <https://doi.org/>

Received:
Accepted:
Published:

Keywords: Electric vehicles; charging scheduling; state-of-charge dependent maximum charging power; mixed integer linear programming.

Publisher's Note: MDPI stays neutral with regard to jurisdictional claims in published maps and institutional affiliations.

Copyright: © 2021 by the authors. Submitted to *Energies* for possible open access publication under the terms and conditions of the Creative Commons Attribution (CC BY) license (<https://creativecommons.org/licenses/by/4.0/>).

1. Introduction

The number of electric vehicles (EVs) is rapidly increasing. At the end of 2020, there were around 10 million EVs on the world's roads and the number of EV registrations increased by 41% in 2020 [1]. The uncontrolled charging of this rising number of EVs, together with an increasing share of renewable energy, imposes significant challenges for the stable operation of the power grid in terms of power quality, voltage stability, peak demand, and reliability [2]. Besides further measures, like time-of-use prices [3] or dynamic pricing schemes [4], smart charging [5,6] is considered a promising strategy to mitigate these issues. Smart charging refers to the coordination of the charging of a number of EVs in an intelligent way. Numerous approaches for smart charging,

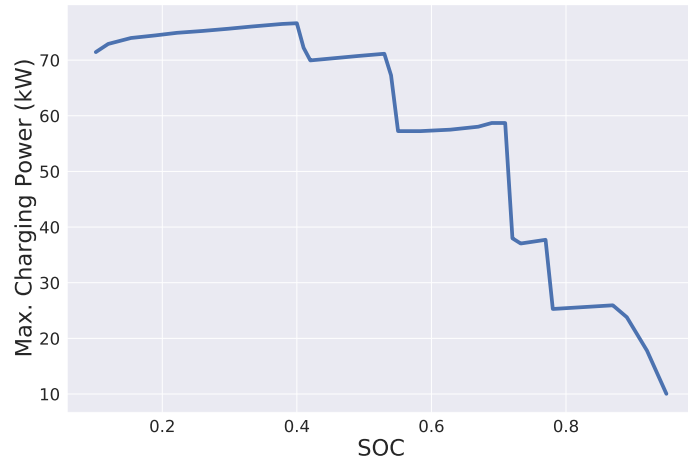


Figure 1. Maximum charging power of a Hyundai Kona Elektro in dependence of the EV's SOC; data obtained from Fastned [15].

37 considering different objectives and different constraints, are proposed in the literature
38 [7–14].

39 These approaches typically assume that the maximum charging power of an EV
40 remains constant over the planning horizon. However, in practice the maximum charging
41 power depends on the state of charge (SOC) of the EV's battery. Typically, with an
42 increasing SOC, the maximum charging power is regulated down by the battery controller.
43 For slow AC charging, the decrease of the maximum power is usually only marginal and
44 can be neglected for most applications. For modern fast DC charging, however, the effect
45 of the decreasing maximum power can be substantial as can be seen from the exemplary
46 SOC-power curve shown in Figure 1. The exact form of the curve does not only depend on
47 the type of battery and its charging controller but also on other factors like the ambient
48 temperature or the state of health of the battery [16]. In most cases the curve is highly
49 nonlinear, making it difficult to consider it in mixed integer linear programming (MILP)
50 approaches, which are frequently used for charging planning. However, not considering
51 the SOC-dependent maximum charging power in the charging planning is likely to result
52 in suboptimal or even infeasible charging schedules, especially in the case of fast charging.
53 For example, Frendo et al. [17] conclude from numerical experiments that under the
54 constraint of a limited total charging power, up to 21% more energy can be charged if
55 the SOC-dependent maximum charging power is considered in the planning, compared to
56 not considering it. Frendo et al. also point out that in the literature on smart charging,
57 the integration of nonlinear SOC-power curves is frequently mentioned as future work.
58 However, to date the number of works, which actually address this issue, is still strongly
59 limited.

60 In the present paper, we assume a basic use case of smart charging with the objective
61 of minimizing the energy cost under time-varying electricity prices and with the constraint
62 of a limited total charging power per time step. In order to allow a better integration of
63 nonlinear SOC-power curves, we formulate the scheduling problem in terms of planning
64 the charging energy instead of the charging power. Therefore, we consider two approaches
65 for converting the SOC-power curves to SOC-energy curves. The first approach is an
66 exact approach, but it can only guarantee that the *average* total charging power does not
67 exceed the limit in a time step. The second approach is an approximate approach, which
68 guarantees that the total charging power never exceeds the limit, but it might lead to
69 suboptimal costs.

70 We propose two methods for solving the resulting problems. The first one is an
71 extension of a cutting plane method proposed by Korolko and Sahinoglu [18] and utilizes
72 a convex hull of the in general nonconcave SOC-power curves. The second method makes
73 use of a piecewise linearization of the SOC-energy curve and is accelerated by branch-

74 and-cut. In extensive numerical experiments, we evaluate and compare the proposed
75 approaches. The key contributions of the present paper are

- 76 • a reformulation of the scheduling problem in terms of the control of charging energy,
77 which facilitates the integration of SOC-dependent maximum charging power,
- 78 • a proposal of two transformations of SOC-power curves into SOC-energy curves,
- 79 • and a proposal and evaluation of two mixed integer linear programming based
80 solution methods that consider SOC-dependent maximum charging powers.

81 Note that the current work is based on parts of Schaden's master thesis [19], where more
82 details and further results can be found. The rest of the paper is organized as follows.
83 The next section discusses related work. In Section 3 our EV charging scheduling problem
84 is formalized. Additionally, it is shown how to derive the exact as well as an approximate
85 maximum charging energy function from the maximum charging power function. Next,
86 Section 4 presents the different problem solving approaches. Section 5 explains how we
87 generated problem instances for the empirical evaluation, and respective experimental
88 results are presented in Section 6. Finally, Section 7 concludes this work and outlines
89 promising future research directions.

90 2. Related Work

91 Some works consider a SOC-dependent maximum charging power by integrating
92 nonlinear physical battery models in the charging schedule optimization. Sundström
93 and Binding [20] compare the use of a linear and a quadratic approximation of such a
94 model in the optimization of EV schedules with the goal of minimizing charging costs.
95 They conclude that although the linear approximation results in small violations in
96 SOC's requested by the EV drivers, the benefit of the quadratic approximation does not
97 justify the increase in computation time. Morstyn et al. [21] propose a nonlinear battery
98 circuit model and integrate it in an optimization model in form of a second-order cone
99 program. They consider the maximization of charged energy taking into account network
100 constraints and the constraints of a limited total charging power. It is shown that problem
101 instances with up to 500 vehicles can be solved within less than 100 seconds. In practice,
102 the behavior of the battery (controller) can significantly differ from an idealized battery
103 model. Thus, other works – including the present work – abstract from a specific battery
104 model.

105 Different battery model-free heuristic approaches for smart charging with SOC-
106 dependent maximum power can be found in the literature. Cao et al. [22] propose a
107 rule-based approach for EV charging control with the objectives of energy cost reduction
108 and load flattening, respecting the SOC-dependent maximum charging powers of EVs.
109 Frendo et al. [17] describe the use of a data-driven approach for the prediction of power
110 curves of EVs. The authors propose a rule-based control, which schedules the charging
111 of the EVs with the objective of a fair distribution of the available energy taking into
112 account the predicted power curves.

113 El-Bayeh et al. [23] propose a model-free exact approach. They approximate a
114 nonlinear power curve with a piecewise linear function. Subsequently, they draw a
115 comparison between the charging costs resulting from charging with a constant maximum
116 charging power and the charging costs resulting from charging with a vehicle specific
117 SOC-dependent piecewise linear function. For solving the optimization problem, they
118 use mixed integer nonlinear programming, which distinguishes their approach from our
119 problem solving techniques. Han, Park, and Lee [24] consider a problem setting similar to
120 that considered in the present paper. The authors assume that the charging station has
121 limited grid capacity, which may be exceeded at the price of paying penalty costs. They
122 present a MILP formulation of the problem, which integrates nonlinear power curves
123 with help of a discretization of SOC levels. In contrast to the present work, it is assumed
124 that EVs can only charge with maximum or zero power, which is quite restrictive and
125 hardly the case in practice. Two network flow approaches in Schaden's Master thesis [19]
126 extend the MILP formulation from [24] with the possibility to charge with power levels

127 from a discrete set of values. However, we refrain from considering these approaches here
 128 as they have been found to be uncompetitive, primarily due to the much larger memory
 129 requirements even when the number of EVs is low.

130 A further model-free exact approach is proposed by Korolko and Sahinoglu [18].
 131 They assume a problem setting similar to that considered in [24] but with continuous
 132 charging power values. A nonlinear problem formulation is presented and is solved as
 133 a series of linear problems with the help of a cutting plane approach. The described
 134 approach, however, requires the power curve to be concave. Our approaches partly build
 135 upon this work.

136 The approaches proposed in the present paper, are model-free linear exact approaches
 137 for a continuous power modulation, which are applicable to concave and nonconcave
 138 power curves. None of the previous works considers the issue that the variable maximum
 139 charging power varies within a time step of the planning horizon. To the best of our
 140 knowledge, we are the first considering this aspect in more detail.

141 3. Problem Description

142 The EV charging scheduling problem with SOC-dependent maximum charging power
 143 (EVS-SOC) we consider formalizes the task of scheduling the charging of a number of EVs
 144 such that the total charging costs are minimized. The charging schedule is preemptive,
 145 which means that the charging process of an EV may be interrupted an arbitrary number
 146 of times. It is assumed that electricity costs change over time and that they are known in
 147 advance. Discrete finite time steps $T = \{0, \dots, t_{\max}\}$ are used to model the considered
 148 time horizon. Each of these represents a time interval of constant duration Δt .

149 The charging is controlled by a single central entity, the so-called aggregator. The
 150 total power that can be used from the grid at any time is limited by $P^{\text{gridmax}} > 0$.
 151 Electricity costs per unit of consumed energy are given by c_t individually for each time
 152 step $t \in T$. Note that these costs may also be negative in practice.

153 The set of EVs to be considered is $V = \{1, \dots, n\}$, and they are all assumed to
 154 be currently connected to the charging station, i.e., immediately available for charging.
 155 Each vehicle is associated with an initial state of charge $s_{v,0} \in [0, 1]$, i.e., the SOC
 156 at the beginning of time step zero, and a minimum required state $s_v^{\text{dep}} \in [s_{v,0}, 1]$ that
 157 must be reached at the vehicle's known departure time $t_v^{\text{dep}} \in T$. Additionally, for each
 158 vehicle $v \in V$ the energy capacity $C_v > 0$ of its battery is known as well as a function
 159 $P_v^{\text{max}} : [0, 1] \mapsto \mathbb{R}^+$ for the battery's maximum charging power given its SOC. Note
 160 that P_v^{max} must be strictly positive for any SOC less than one and is zero for SOC one.
 161 Otherwise we do not restrict this function in any way, in particular it does not necessarily
 162 have to be concave or continuous. Note that we neglect the effect of minor further factors
 163 like the battery temperature and its state of health on the maximum charging power.
 164 Furthermore, we assume a charging efficiency of 100%.

165 We remark that in practice, the domain of P_v^{max} is often not defined on the entire
 166 SOC interval $[0, 1]$ but just for some restricted $[s_v^{\text{min}}, s_v^{\text{max}}]$, $0 \leq s_v^{\text{min}} < s_v^{\text{max}} \leq 1$. In the
 167 following, we will regard this issue as an implementation detail and assume the domain
 168 of P_v^{max} to be $[0, 1]$.

169 The goal of EVS-SOC is to find a feasible charging schedule that minimizes the total
 170 charging costs while charging each vehicle v from SOC $s_{v,0}$ to (at least) SOC s_v^{dep} by
 171 time step t_v^{dep} such that the total power used from the grid at any time does not exceed
 172 $P^{\text{gridmax}} > 0$.

173 Since the maximum charging power function P_v^{max} depends on the SOC, it is in
 174 general not constant within a single time step of duration Δt . This may lead to the
 175 problem that a charging power value set for a time step is not allowed throughout the
 176 whole charging interval. The vehicle's charging controller will then dynamically adjust
 177 (reduce) the actually used power to never exceed the SOC-dependent maximum power.
 178 One may argue that the resulting error may be reduced by increasing the resolution of the
 179 time discretization until it becomes negligible. A larger number of time steps, however,

180 directly affects the problem size and practical solvability. Therefore, we refrain here from
181 increasing t_{\max} only because of this reason.

182 Instead, we turn from considering the charging power to considering the energy by
183 which an EV may actually be charged in a time step, taking care of the above aspects. We
184 propose alternative approaches for deducing an (approximate) maximum energy function
185 $E_v^{\max}(s) : [0, 1] \mapsto \mathbb{R}^+$ from P_v^{\max} that states the maximum energy by which EV v with
186 SOC s can be charged within duration Δt .

187 In Section 3.1 we give an exact way for deducing E_v^{\max} , referred to as $E_v^{\max\text{-ex}}$.
188 However, using $E_v^{\max\text{-ex}}$, we are in general only able to express that the maximum grid
189 power is not exceeded *on average* within a time step, since we consider the time horizon
190 in a discretized fashion. While this might be sufficient for some applications, like limiting
191 peak load charges, it may be a too weak condition for other applications, like limiting
192 transformer loads. Therefore, in Section 3.2 we also show how to deduce a lower bound
193 $E_v^{\max\text{-lb}}$ to E_v^{\max} that never overestimates the real maximum energy at which charging
194 can take place.

195 3.1. Exact Maximum Energy

We determine the maximum charging energy $E_v^{\max\text{-ex}}$ that is achieved when applying
the dynamic charging power P_v^{\max} throughout a whole time step. Considering an EV
 $v \in V$ with initial SOC $s_{v,t} \in [0, 1]$ at some time step $t \in \{0, \dots, t_v^{\text{dep}} - 1\}$, the time
needed to charge the EV to some SOC $s' \in [s_{v,t}, 1]$ using the dynamic maximum charging
power is

$$T_v^{\text{min-ex}}(s_{v,t}, s') = C_v \cdot \int_{s_{v,t}}^{s'} \frac{1}{P_v^{\max}(s)} ds. \quad (1)$$

The maximum energy by which the EV can be charged during a time step of duration Δt
is then

$$E_v^{\max\text{-ex}}(s_{v,t}) = C_v \cdot (s' - s_{v,t}) \text{ s.t. } \begin{cases} T_v^{\text{min-ex}}(s_{v,t}, s') = \Delta t & \text{for } T_v^{\text{min-ex}}(s_{v,t}, 1) > \Delta t \\ s' = 1 & \text{else.} \end{cases} \quad (2)$$

196 Hereby we consider in the else case that charging always stops when SOC value one is
197 reached. While calculating the integral for $\frac{1}{P_v^{\max}(s)}$ might be nontrivial from a theoretical
198 point-of-view for some power functions, it is in practice not difficult to efficiently determine
199 approximate values for $E_v^{\max\text{-ex}}(s_{v,t})$ computationally by conventional numerical integra-
200 tion methods. As previously mentioned, the problem with the usage of $E_v^{\max\text{-ex}}(s_{v,t})$ is
201 primarily that it is hard to express the maximum grid power constraint since within a
202 time step the actually used power may vary for each EV substantially, i.e., we will only
203 be able to express that the maximum grid power is not exceeded *on average* within a
204 time step.

205 3.2. Lower Bound for Maximum Energy

To address the aforementioned problem, we consider the largest power that can be
constantly applied throughout a whole time step of duration Δt without requiring the
charging controller to reduce the power. The time needed to charge the EV to some SOC
 $s' \in [s_{v,t}, 1]$ using the maximum power that can be constantly applied is

$$T_v^{\text{min-lb}}(s_{v,t}, s') = \frac{C_v \cdot (s' - s_{v,t})}{\min_{s \in [s_{v,t}, s']} P_v^{\max}(s)}. \quad (3)$$

206 The maximum energy by which the EV can be charged during a time step of duration Δt
207 is then again obtained by Eq. (2) but in conjunction with the above $T_v^{\text{min-lb}}$ (3) instead
208 of $T_v^{\text{min-ex}}$ (1). We refer to this variant by $E_v^{\max\text{-lb}}$.

209 By avoiding to set for a time step a power that will have to be reduced by the
210 charging controller at some point of time, the maximum energy $E_v^{\max\text{-lb}}$ is a lower bound

211 for the actually obtainable energy $E_v^{\max\text{-ex}}$. Using $E_v^{\max\text{-lb}}$ in our whole problem setting
 212 means that an obtained solution will guarantee that indeed all EVs are charged to the
 213 desired departure SOC. As we may occasionally use a more restricted charging power
 214 than could actually be applied, the schedule might not be optimal in the original sense,
 215 and a solution's objective value will be an upper bound for the real optimum.

216 We want to point out the following relationships between P_v^{\max} and its corresponding
 217 maximum energy functions.

- 218 • If P_v^{\max} is a piecewise linear function, then $E_v^{\max\text{-lb}}$ is piecewise linear as well. On the
 219 contrary, $E_v^{\max\text{-ex}}$ might not be a piecewise linear function, even if P_v^{\max} is piecewise
 220 linear.
- 221 • If P_v^{\max} is a concave function, so are $E_v^{\max\text{-lb}}$ and $E_v^{\max\text{-ex}}$.

222 To give the reader an impression how $E_v^{\max\text{-lb}}$ and $E_v^{\max\text{-ex}}$ relate to each other,
 223 Figure 2 shows these functions for different Δt values for a Hyundai Kona Elektro. Note
 224 that the area between $E_v^{\max\text{-lb}}$ and $E_v^{\max\text{-ex}}$ decreases with smaller Δt values. Hence, as
 225 we will also see in Section 6, the smaller Δt is chosen, the smaller will be the size of the
 error introduced by $E_v^{\max\text{-lb}}$ in general.

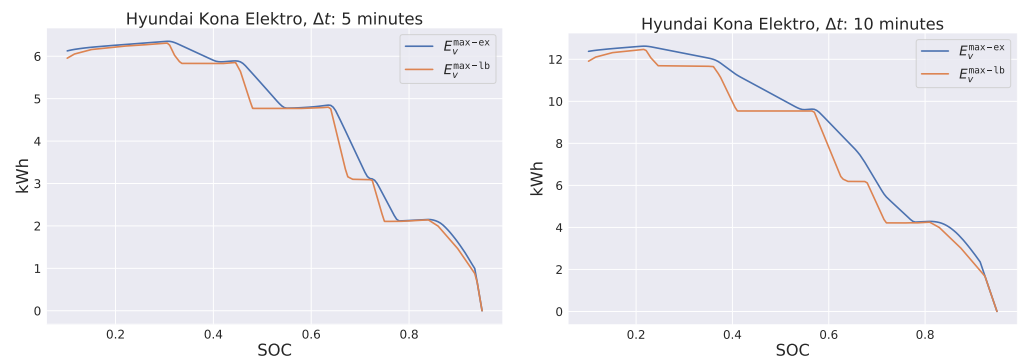


Figure 2. E_v^{\max} functions for a Hyundai Kona Elektro for $\Delta t \in \{5, 10\}$ minutes.

226 In the following sections we will pursue $E_v^{\max\text{-ex}}$ and $E_v^{\max\text{-lb}}$ and investigate the
 227 pros and cons of each in comparison. We will use the notation E_v^{\max} as a placeholder for
 228 any specific energy function from $\{E_v^{\max\text{-ex}}, E_v^{\max\text{-lb}}\}$.
 229

230 3.3. Converting Energy Back to Power

231 In practice, the charging aggregator usually regulates the maximum charging *power*
 232 instead of the maximum charging *energy*. Consequently, when scheduling with energy
 233 values we have to convert back energy values to power values. For schedules created with
 234 $E_v^{\max\text{-lb}}$, the computed energy values of a schedule can be simply divided by Δt to obtain
 235 charging power values that can be constantly applied throughout a single time step.

For schedules created with the exact $E_v^{\max\text{-ex}}$, due to the possible interference of
 the EV's charging controller it is in general not obvious which power value $P_{v,t}$ should
 be provided to the charging aggregator in order to actually charge a certain amount of
 energy $x_{v,t}$ in a next time step t . Considering $P_v^{\max}(s)$, this value $P_{v,t}$ can be determined
 computationally by numerically solving the equation

$$236 \quad C_v \cdot \int_{s_{v,t}}^{s_{v,t} + x_{v,t}/C_v} \frac{1}{\min(P_v^{\max}(s), P_{v,t})} ds = \Delta t, \quad (4)$$

237 where the left side corresponds to the time needed for charging $x_{v,t}$ when applying as
 238 power always the minimum of $P_v^{\max}(s)$ and $P_{v,t}$. Still there remains the issue that in
 239 a solution to our scheduling problem $\sum_{v \in V} P_{v,t} \leq P^{\text{gridmax}}$ is not guaranteed anymore
 240 and either P^{gridmax} may be exceeded or some $P_{v,t}$ needs to be reduced to avoid this
 241 problem. Note that Equation (4) is well defined for all $x_{v,t} \in [0, C_v(s' - s_{v,t})]$ where s' is
 determined according to Equation (2).

242 Therefore, schedules created with $E_v^{\max\text{-ex}}$ mainly serve here as comparison for
 243 schedules created with $E_v^{\max\text{-lb}}$ to give an idea about the size of the error introduced by
 244 time discretization.

245 3.4. Nonlinear Model

We now formally define EVS-SOC by the following nonlinear program, where variables $x_{v,t}$ represent the energy by which EV $v \in V$ is charged in time step $t = 0, \dots, t_v^{\text{dep}} - 1$. Variables $s_{v,t}$ indicate the SOC of each EV $v \in V$ at the beginning of each time step $t = 0, \dots, t_v^{\text{dep}}$.

$$\min \sum_{v \in V} \sum_{t=0}^{t_v^{\text{dep}}-1} c_t \cdot x_{v,t} \quad (5)$$

$$x_{v,t} \leq E_v^{\max}(s_{v,t}) \quad v \in V, t = 0, \dots, t_v^{\text{dep}} - 1 \quad (6)$$

$$\sum_{v \in V | 0 \leq t < t_v^{\text{dep}}} x_{v,t} \leq \Delta t \cdot P^{\text{gridmax}} \quad t \in T \quad (7)$$

$$s_v^{\text{dep}} \leq s_{v,t_v^{\text{dep}}} \quad v \in V \quad (8)$$

$$s_{v,t} = s_{v,t-1} + x_{v,t-1}/C_v \quad v \in V, t = 1, \dots, t_v^{\text{dep}} \quad (9)$$

$$x_{v,t} \geq 0 \quad v \in V, t = 0, \dots, t_v^{\text{dep}} - 1 \quad (10)$$

$$0 \leq s_{v,t} \leq 1 \quad v \in V, t = 0, \dots, t_v^{\text{dep}} \quad (11)$$

246 The objective function (5) minimizes the sum of the costs for the total consumed
 247 energy over all time steps. Inequalities (6) ensure that the energy by which each EV is
 248 charged during each time step does not exceed the SOC-dependent maximum energy.
 249 Note that this inequality is in general nonlinear. Constraints (7) limit the total energy
 250 consumed from the grid during each time step to $\Delta t \cdot P^{\text{gridmax}}$. The departure SOCs are
 251 enforced by Inequalities (8). Equalities (9) determine the SOC at the beginning of each
 252 time step $t = 1, \dots, t_v^{\text{dep}}$ for each EV v . Thereunto the previous state of charge $s_{v,t-1}$ is
 253 considered together with the charging rate of the previous time slot $x_{v,t-1}$ and the total
 254 battery capacity C_v . Variable domains are defined in (10) and (11). Due to the domain
 255 of variable $x_{v,t}$, an EV may not discharge.

256 4. Problem Solving Approaches

257 In the following we study different ways to deal with the nonlinear maximum
 258 charging energy constraints (6). We first consider the simpler case that the maximum
 259 power function is concave, where we essentially can solve the problem with a linear
 260 programming (LP) formulation or a cutting plane approach. Afterwards, we consider
 261 a more general approach that does not make any assumptions on the concavity of the
 262 maximum power function. The approach is based on a piecewise linearization of the
 263 SOC-energy curve and is accelerated by branch-and-cut.

264 4.1. Concave Maximum Energy Functions

265 As already mentioned before, if P_v^{\max} is concave, it follows that also $E_v^{\max} \in$
 266 $\{E_v^{\max\text{-ex}}, E_v^{\max\text{-lb}}\}$ is concave as well. For nonconcave P_v^{\max} , we now determine the
 267 convex hull to obtain a concave approximation of the original P_v^{\max} for deriving the
 268 respective maximum energy function.

269 In the following, we will further assume that E_v^{\max} is differentiable. We are aware
 270 that, depending on P_v^{\max} , this assumption might not be completely valid in practice.
 271 Actually, E_v^{\max} might have breakpoints, in which the left-sided and right-sided limits of
 272 the differential do not coincide. Nevertheless, we will treat E_v^{\max} as if it were differentiable
 273 at any SOC of its domain, since differing left-sided and right-sided limits will not affect
 274 the results of the following modeling approach.

Due to the assumed properties of E_v^{\max} , we can replace the nonlinear Inequality (6) from EVS-SOC with the combination of the infinite set of linear inequalities

$$x_{v,t} \leq E_v^{\max'}(\hat{s}) \cdot (s_{v,t} - \hat{s}) + E_v^{\max}(\hat{s}) \quad v \in V, t = 0, \dots, t_v^{\text{dep}} - 1, \hat{s} \in [s_{v,0}, s_v^{\text{dep}}] \quad (12)$$

where $E_v^{\max'}$ is the first derivative of E_v^{\max} . We call the resulting linear programming model EVS-SOC-LIN.

Note that if P_v^{\max} is a piecewise linear function, then so is $E_v^{\max\text{-lb}}$. The set of inequalities reduces then to a finite one where we have one inequality corresponding to each linear function segment.

In the spirit of [18], who essentially consider a similar kind of inequalities, we can solve EVS-SOC-LIN by a cutting plane approach. Thereby the relaxation of EVS-SOC-LIN without Inequalities (12) is first solved. Then, Inequalities (12) that are violated by the current LP solution are iteratively determined, added, and the LP problem is re-solved. The process is repeated until no more Inequalities (12) are violated.

The separation of a violated inequality for a current solution $(x^{\text{LP}}, s^{\text{LP}})$ to the relaxed EVS-SOC-LIN works as follows. For all $v \in V$, $t = 0, \dots, t_v^{\text{dep}} - 1$, we check if $x_{v,t}^{\text{LP}} > E_v^{\max}(s_{v,t}^{\text{LP}})$. In this case we add the violated Inequality (12) for vehicle v , time step t , and $\hat{s} = s_{v,t}^{\text{LP}}$. Note that for one vehicle, multiple inequalities for different time steps can be added within a single cutting plane iteration. This separation procedure is performed for all vehicles $v \in V$ and as long as any violated inequalities are found, the augmented LP problem is then re-solved.

An alternative to the above is the following. Whenever $x_{v,t}^{\text{LP}} > E_v^{\max}(s_{v,t}^{\text{LP}})$ for some EV v and time step t , one can add the violated Inequality (12) not only for time step t but for all time steps $t' = 0, \dots, t_v^{\text{dep}} - 1$. The intention here is to possibly reduce the number of needed resolving iterations, but clearly the size of the LP formulation increases more quickly. Preliminary experiments indicated that indeed this variant performs better in practice in most cases. Therefore, we apply it in all our experiments documented in the remainder of this work.

We also compared this variant with the approach presented in [18], where in one iteration cuts are only added for the smallest time steps that violate Inequality (12). We found that our variant usually performs slightly better at least in case of our problem instances.

4.2. General Piecewise Linear Maximum Energy Functions

In the following model, we assume for each EV $v \in V$ that the maximum charging energy function E_v^{\max} is a piecewise linear function or is approximated by such. In contrast to EVS-SOC-LIN, we do not make assumptions on the concavity of E_v^{\max} . We assume that we are given a finite set of SOC values $\{S_{v,k} \mid k = 1, \dots, k_v^{\max}\}$ in increasingly sorted order, with $S_{v,1} = 0$ and $S_{v,k_v^{\max}} = 1$ and the values in between representing the breakpoints of the piecewise linear function. These values are pairwise distinct and can be unevenly distributed among the SOC interval $[0, 1]$. For each $S_{v,k}$ we know the value of the maximum charging energy $E_v^{\max}(S_{v,k})$.

We model the piecewise linear function as suggested in Chapter 10.1 of [25]. Thereunto, we use continuous variables $\alpha_{v,t,k}$ to express the SOC $s_{v,t}$ as a convex combination of $S_{v,k}$ and $\alpha_{v,t,k}$. The variables $\alpha_{v,t,k}$ are also used to represent the maximum charging energy function as a convex combination of $E_v^{\max}(S_{v,k})$ and $\alpha_{v,t,k}$.

Furthermore, we introduce additional binary variables $\beta_{v,t,k}$, which are used to ensure that at most two consecutive $\alpha_{v,t,k}$ and $\alpha_{v,t,k+1}$ variables are nonzero. By replacing Constraints (6) in formulation (5–11) with the following Constraints (13–21), we obtain a MILP model, which we refer to as EVS-SOC-GLIN.

$$s_{v,t} = \sum_{k=1}^{k_v^{\max}} S_{v,k} \cdot \alpha_{v,t,k} \quad v \in V, t = 0, \dots, t_v^{\text{dep}} \quad (13)$$

$$x_{v,t} \leq \sum_{k=1}^{k_v^{\max}} E_v^{\max}(S_{v,k}) \cdot \alpha_{v,t,k} \quad v \in V, t = 0, \dots, t_v^{\text{dep}} - 1 \quad (14)$$

$$\sum_{k=1}^{k_v^{\max}} \alpha_{v,t,k} = 1 \quad v \in V, t = 0, \dots, t_v^{\text{dep}} \quad (15)$$

$$\sum_{k=1}^{k_v^{\max}-1} \beta_{v,t,k} = 1 \quad v \in V, t = 0, \dots, t_v^{\text{dep}} \quad (16)$$

$$\alpha_{v,t,0} \leq \beta_{v,t,0} \quad v \in V, t = 0, \dots, t_v^{\text{dep}} \quad (17)$$

$$\alpha_{v,t,k} \leq \beta_{v,t,k-1} + \beta_{v,t,k} \quad v \in V, t = 0, \dots, t_v^{\text{dep}}, k = 2, \dots, k_v^{\max} - 1 \quad (18)$$

$$\alpha_{v,t,k_v^{\max}} \leq \beta_{v,t,k_v^{\max}-1} \quad v \in V, t = 0, \dots, t_v^{\text{dep}} \quad (19)$$

$$0 \leq \alpha_{v,t,k} \leq 1 \quad v \in V, t = 0, \dots, t_v^{\text{dep}}, k = 1, \dots, k_v^{\max} \quad (20)$$

$$\beta_{v,t,k} \in \{0, 1\} \quad v \in V, t = 0, \dots, t_v^{\text{dep}}, k = 1, \dots, k_v^{\max} - 1 \quad (21)$$

Equations (13) link the SOC values $s_{v,t}$ with the continuous weight variables $\alpha_{v,t,k}$. The charging energy $x_{v,t}$ of EV v at time slot t is limited by Inequalities (14) to the maximum charging energy. Constraints (15) set the sum of the continuous weights $\alpha_{v,t,k}$ over all discrete SOC levels $k = 1, \dots, k_v^{\max}$ to one. Equations (16) ensure that exactly one $\beta_{v,t,k}$ variable is active for each EV v and time slot t . The $\alpha_{v,t,k}$ variables are linked with the $\beta_{v,t,k}$ variables by Inequalities (17–19). Altogether, (16–19) are the so-called adjacency constraints, which ensure that at most two consecutive variables $\alpha_{v,t,k}$ and $\alpha_{v,t,k+1}$ are nonzero. Constraints (20–21) define the domains of $\alpha_{v,t,k}$ and $\beta_{v,t,k}$, respectively.

As we will see in Section 6, the previously introduced EVS-SOC-LIN formulation, which requires E_v^{\max} to be concave, performs remarkably well. Therefore, we propose a branch-and-cut approach for solving EVS-SOC-GLIN, in which we initially work on the convex hull of $\{(S_{v,k}, E_v^{\max}(S_{v,k})) \mid k = 1, \dots, k_v^{\max}\} \cup \{(S_{v,1}, 0), (S_{v,k_v^{\max}}, 0)\}$. To obtain this relaxation, we consider the original EVS-SOC-GLIN formulation with all its variables and constraints except the linking constraints (17–19). Then, whenever a solution candidate is found, we check for all $v \in V, t = 0, \dots, t_v^{\text{dep}} - 1$ whether $x_{v,t}$ exceeds the actual E_v^{\max} value at SOC $s_{v,t}$, i.e., if $x_{v,t} > E_v^{\max}(s_{v,t})$. If this is the case, a cut is added that links all nonzero $\alpha_{v,t,k}$ variables with their respective $\beta_{v,t,k}$ variables, as we did in Constraints 17–19. Such cuts are separated and added until for all $v \in V, t = 0, \dots, t_v^{\text{dep}} - 1$ it holds that $x_{v,t} \leq E_v^{\max}(s_{v,t})$.

5. Benchmark Instances

Due to the lack of pure real-world problem instances we randomly generate benchmark instances and use real-world data as far as possible. Specifically, battery capacities and maximum power functions are adopted from real-world data. We first consider individual EVS-SOC instances that represent snapshot scenarios at certain times with a specific number of vehicles that are assumed to have arrived at the charging station following a homogenous Poisson process. Afterwards, in Section 5.2, we will consider whole model based predictive control scenarios with a rolling horizon in which vehicles arrive at different times of a day.

All of the benchmark instances are available at <https://www.ac.tuwien.ac.at/research/problem-instances/>.

EV Name	C_v (kWh)	s_v^{\min}	s_v^{\max}	$\#P_v^{\max}$ -lin. pieces
Energica Ego	21.5	1.1	99.9	53
MINI Cooper Electric	32.6	12.1	93.8	34
BMW i3	42.2	15.1	96.0	26
Hyundai Kona Elektro	67.5	10.1	94.9	28
Tesla Model 3 Long Range	82.0	11.1	99.0	35
Mercedes-Benz EQC	85.0	2.1	97.8	24
Jaguar I-Pace	90.0	8.0	100.0	29
Audi e-tron	95.0	3.1	99.8	44

Table 1: Used EV types with battery capacity C_v , P_v^{\max} domain $[s_v^{\min}, s_v^{\max}]$ and the number of linear pieces of P_v^{\max} .

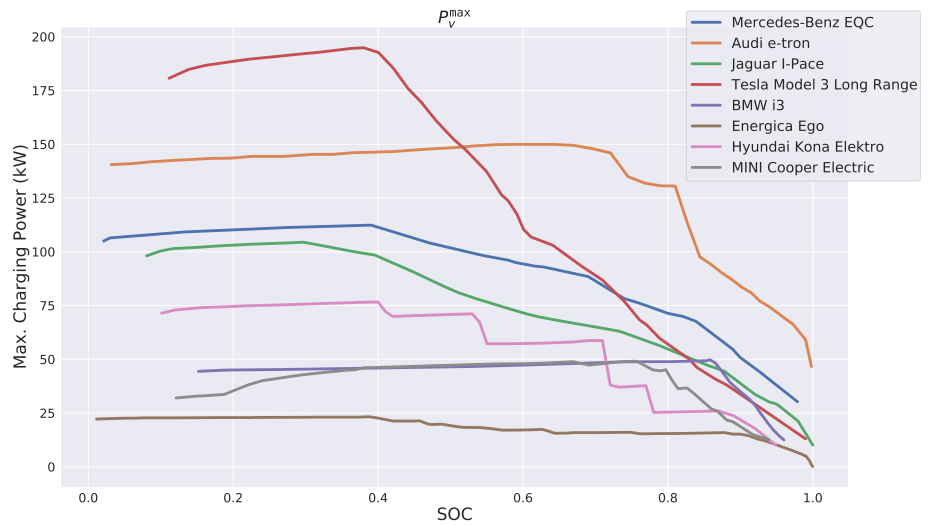


Figure 3. Maximum charging power functions P_v^{\max} for all considered vehicle types.

351 5.1. Individual EVS-SOC Instances

352 We distinguish between three types of problem parameters, depending on whether
 353 the parameter is set by the user, randomly generated, or based on real-world data. To the
 354 input provided by the user, we count the number n of EVs, the length Δt of a time step,
 355 and the grid's power capacity P_{gridmax} . We generate 30 instances for each combination
 356 of $n \in \{10, 20, 50, 100\}$, $\Delta t \in \{1, 5, 10\}$ minutes, and $P_{\text{gridmax}} \in \{10n, 25n, 40n\}$.

357 We consider eight different types of real EVs shown in Table 1. The EV's battery
 358 capacities were taken from the EV Database¹. The respective maximum power functions
 359 P_v^{\max} were manually extracted from plots found on the website of the Dutch EV charging
 360 station operator FASTNED². More specifically, 25 up to 70 points of a plot were manually
 361 determined in dependence of notable changes of the gradient, and linear interpolation
 362 was applied in between. All these P_v^{\max} functions are shown in Figure 3. Observe that
 363 the maximum power function's available domain of definition $[s_v^{\min}, s_v^{\max}]$ varies among
 364 the EVs. If a vehicle type supports speed charging, the respective most powerful charging
 365 curve is used.

366 Since the P_v^{\max} data extracted from the original plots is quite fine-grained, we
 367 additionally derive simplified piecewise linear approximations with only five and ten
 368 linear pieces, respectively. For this task, we utilized the Python package `pwlf` [26] to
 369 determine approximately optimal breakpoints automatically.

370 A comparison between the original P_v^{\max} and these simpler piecewise approximations
 371 is shown in Figure 4 exemplarily for the Hyundai Kona Elektro. Observe that the

¹ <https://www.ev-database.de>

² <https://fastnedcharging.com>

372 approximation of the original P_v^{\max} function with 10 segments is already quite good for
 373 this rather challenging vehicle type. For P_v^{\max} of the other vehicle types, see Appendix
 374 A.

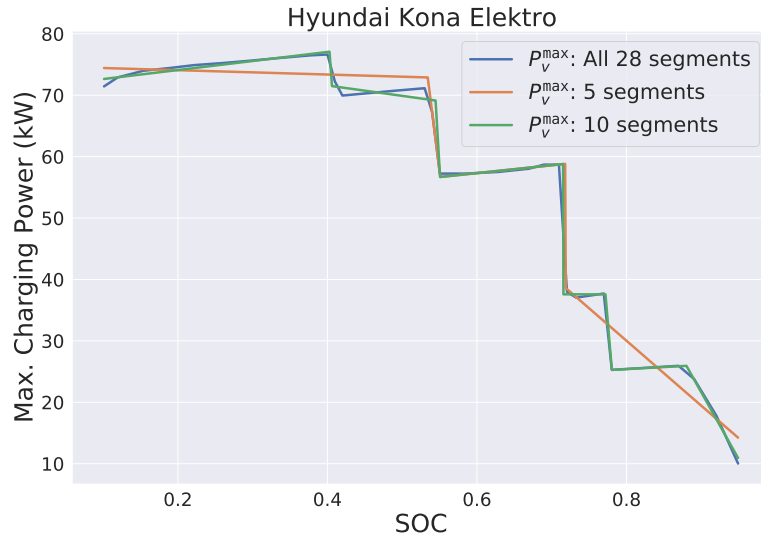


Figure 4. Exemplary P_v^{\max} curve with different number of segments.

375 For each EV $v \in V$ in a benchmark instance, one of the above EV types is chosen
 376 uniformly at random. Moreover, we choose an availability duration at the charging
 377 station d_v^{avail} randomly according to a normal distribution with a mean value of six hours
 378 and a standard deviation of 1.5 hours.

Next, from the interval $(-d_v^{\text{avail}}/\Delta t, 0)$ we select an arrival time t_v^{arr} uniformly at
 random and obtain a respective departure time $t_v^{\text{dep}} = \lceil t_v^{\text{arr}} + d_v^{\text{avail}}/\Delta t \rceil$. Considering
 the available domains of definition of the maximum power functions, we generally assume
 that each vehicle shall be charged from a SOC of 20% at arrival to a SOC of 90% at
 departure. In our benchmark instances, we therefore choose the initial SOC proportional
 to the already bygone availability time, i.e., for all $v \in V$,

$$s_{v,0} = \frac{-t_v^{\text{arr}}}{d_v^{\text{avail}}/\Delta t} \cdot 0.7 + 0.2. \quad (22)$$

379 The departure SOC s_v^{dep} is set to 90% for all EVs.

380 The end of the time horizon is obtained from the last EV's departure time, i.e.,
 381 $t_{\max} = \max_{v \in V} t_v^{\text{dep}}$. Electricity costs per unit of consumed energy c_t are independently
 382 chosen for each time step $t \in T$ uniformly at random from [1.9, 3.5) cent/kWh.

383 5.2. Rolling Horizon Benchmark Scenarios

384 In addition to the individual benchmark instances, we consider rolling horizon
 385 simulations over whole days starting at time 0:00 and ending at 24:00. To deal with such
 386 a scenario in which vehicles arrive at different times at the charging station, the schedule
 387 is (re-)optimized at time 0:00 and then every $\tau = 10$ minutes, always considering only
 388 EVs that are currently available at the charging station. The found charging schedule is
 389 then assumed to be applied for the next τ minutes until a new schedule is determined.

390 The time is again discretized into equally long time steps of $\Delta t \in \{5, 10\}$ minutes.
 391 Electricity costs per unit of consumed energy are chosen as explained in Section 5.1 and it
 392 is assumed that they are known in advance for the whole charging period. For the number
 393 of vehicles we use $n \in \{10, 20, 50, 100\}$. Again, we pick each vehicle type uniformly at
 394 random from the set of available vehicle types.

395 It is assumed that most vehicles arrive around two peak times at 6:00 and 14:00.
 396 For picking the arrival time t_v^{arr} for a vehicle $v \in V$, we therefore first randomly select

397 with equal probability one of these two peak times and then sample t_v^{arr} from a normal
 398 distribution with the chosen peak time as mean value and a standard deviation of two
 399 hours. Times outside of the considered horizon of 24 hours are re-sampled.

400 The charging duration d_v^{avail} is chosen as described in Section 5.1 and t_v^{dep} is derived
 401 correspondingly. Also, s_v^{dep} and P^{gridmax} are set as before. At time 0:00 we set $s_{v,0} = 0.2$
 402 and with each rescheduling we determine $s_{v,0}$ based on the charging schedule of the
 403 previous iteration.

404 Thirty independent whole-day scenarios were constructed and are considered in the
 405 experimental evaluation.

406 5.2.1. Exemplary Solutions.

407 Figure 5 exemplarily visualizes optimal solutions for a single individual instance
 408 with $n = 5$ EVs and $\Delta t = 5$ minutes obtained from EVS-SOC-GLIN with decreasing
 409 grid power capacity $P^{\text{gridmax}} \in \{50, 125, 200\}$ kW. As maximum energy function we chose
 410 $E_v^{\text{max-lb}}$ based on P_v^{max} with five piecewise linear segments. Each sub-figure represents an
 411 optimal charging schedule of a vehicle fleet. Bars specify the energy a vehicle is charged
 412 with in each time step. The corresponding scale is located on the left y-axis. The grid's
 413 maximum energy supply $P^{\text{gridmax}} \cdot \Delta t$ is indicated as horizontal line in the plots. Crosses
 414 reveal the electricity costs for each time step and the corresponding scale is located on
 415 the right-sided y-axis.

416 For $P^{\text{gridmax}} = 200$ kW it can be observed in Figure 5a that vehicles are charged
 417 usually in parallel within a single time step and cheap electricity costs can be exploited
 418 more effectively. Moreover, at some time steps the charged energy is well below the
 419 grid's power capacity. Figure 5b shows how the charging schedule changes when lowering
 420 P^{gridmax} to 125 kW. By reducing the grid's power capacity, more time steps are required
 421 for charging the vehicles to their target SOC, resulting in higher total charging costs.
 422 Though note that in contrast to the solution shown in Figure 5a, the charging costs only
 423 slightly increase even though the grid's power capacity has been almost halved. When
 424 reducing P^{gridmax} even further to 50 kW, as shown in Figure 5c, the number of time steps
 425 required for charging the vehicles drastically increases. Moreover, in contrast to Figure
 426 5a at most time steps only a single vehicle is charged with usually the maximal possible
 427 energy. Finally, note that independent of the choice of P^{gridmax} the generated solutions
 428 always utilize the time steps at which charging is the cheapest. In summary, Figure 5
 429 shows how the choice of P^{gridmax} affects a respective optimal charging schedule: The
 430 smaller the power capacity of the grid, the more time steps are required for charging the
 431 vehicles and therefore the higher are the total resulting charging costs.

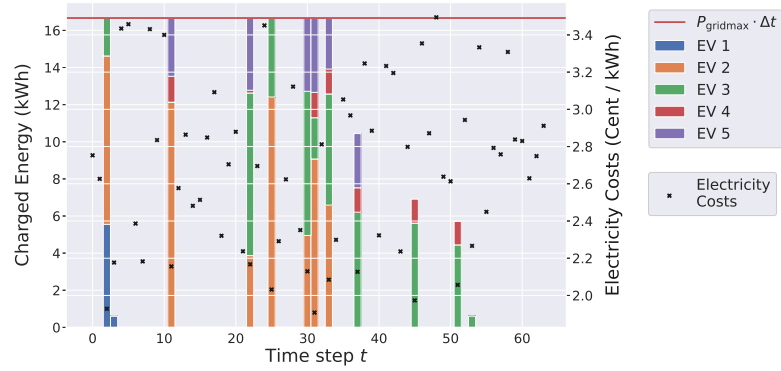
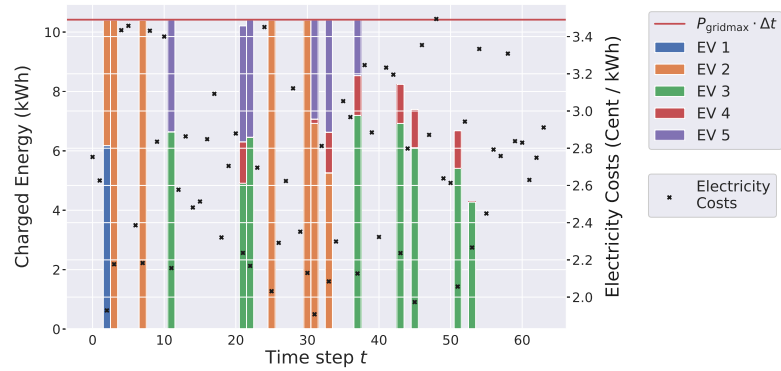
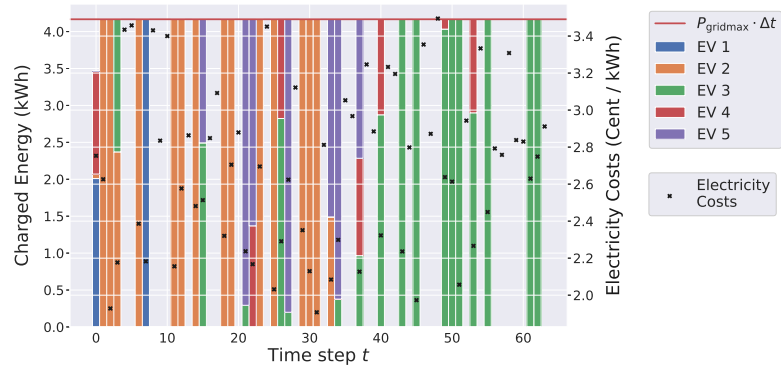
432 6. Experimental Results

433 All solution approaches were implemented in Julia 1.6.0³ using the the optimization
 434 modeling package JuMP v0.21.5 and Gurobi 9.1.0⁴ as LP/MILP solver. Gurobi was
 435 configured to run in single-threaded mode with a time limit of 30 minutes per instance.
 436 All remaining Gurobi parameters were kept at their default values. The experiments were
 437 conducted on an Intel Xeon E5-2640 v4 with 2.40GHz and 16GB memory limit. If not
 438 stated otherwise we report in the following mean or median results on the 30 problem
 439 instances per instance parameter combination $(n, \Delta t, P^{\text{gridmax}}, E_v^{\text{max}})$.

440 We first show individual results for EVS-SOC-LIN and EVS-SOC-GLIN, respectively.
 441 Afterwards, solutions generated by both approaches for the same instances w.r.t. the
 442 same configurations are compared to each other in Section 6.3. Finally, we present results
 443 for the rolling horizon scenarios.

³ <https://julialang.org>

⁴ <https://www.gurobi.com>

(a) $P_{\text{gridmax}} = 200 \text{ kW}$; total charging costs: 290.42 cent.(b) $P_{\text{gridmax}} = 125 \text{ kW}$; total charging costs: 296.91 cent.(c) $P_{\text{gridmax}} = 50 \text{ kW}$; total charging costs: 330.10 cent.**Figure 5.** Optimal solution for an instance with $n = 5$, $\Delta t = 5$ minutes, $P_{\text{gridmax}} \in \{50, 125, 200\} \text{ kW}$ using EVS-SOC-GLIN.444 **6.1. EVS-SOC-LIN**

445 We compare two variants of EVS-SOC-LIN. Recall that for piecewise linear E_v^{max}
 446 only a finite set of inequalities as described by (12) exists. Hence, next to the variant in
 447 which these constraints are dynamically separated as cuts via the cutting plane approach
 448 as described in Section 4.1, we also consider the variant in which all maximum charging
 449 energy constraints (12) are statically added to the LP upfront.

450 The results of this comparison are reported in Table 2. As maximum energy function
 451 $E_v^{\text{max-lb}}$ as well as $E_v^{\text{max-ex}}$ are considered. The energy functions are derived from the
 452 convex hull of P_v^{max} as described in Section 4.1. Moreover, P_{gridmax} is set to $25n$ for
 453 all shown instances. The table lists for each instance group, identified by n and Δt , the
 454 average total number of piecewise linear segments n_{seg} of the E_v^{max} functions over all
 455 vehicles, a comparison of the runtimes between the cutting plane and the static approach,

456 as well as the average total number of added cuts, denoted by n_{cuts} , for the cutting plane
457 approach.

Table 2: EVS-SOC-LIN runtime comparison for concave maximum power functions and $P_{\text{gridmax}} = 25n$: solving the static MILP versus the cutting plane method.

n	Δt (min)	n_{seg}	Runtime (s)				n_{cuts}	
			Static		Cutting Plane		Cutting Plane	
			Mean	Median	StdDev	Median	StdDev	Mean
$E_v^{\text{max-lb}}$								
5	1	49	0.07	0.04	1.34	0.26	10423	5209
5	5	46	0.01	0.00	1.04	0.23	574	269
5	10	43	0.01	0.00	1.03	0.24	190	85
10	1	99	0.18	0.15	1.52	0.38	15949	5580
10	5	93	0.02	0.01	1.05	0.28	1243	520
10	10	86	0.01	0.00	1.03	0.26	416	159
20	1	199	0.60	0.30	2.09	0.49	25549	6715
20	5	187	0.05	0.02	1.10	0.25	2593	747
20	10	172	0.02	0.01	1.05	0.25	862	245
50	1	495	2.78	1.02	6.72	2.07	87375	19749
50	5	464	0.16	0.06	1.28	0.31	6499	1167
50	10	427	0.06	0.02	1.10	0.23	2157	335
100	1	994	9.34	2.60	12.84	3.99	193069	27979
100	5	931	0.56	0.22	1.68	0.32	13502	1664
100	10	858	0.13	0.05	1.25	0.27	4367	475
$E_v^{\text{max-ex}}$								
5	1	901	1.19	1.02	1.31	0.38	12800	5986
5	5	901	0.23	0.11	0.90	0.25	1102	542
5	10	901	0.08	0.07	0.97	0.26	322	205
10	1	1802	4.98	3.27	1.65	0.52	25271	9541
10	5	1802	0.59	0.22	1.06	0.24	2341	950
10	10	1802	0.22	0.10	1.01	0.20	757	387
20	1	3605	14.33	8.48	3.29	0.83	60778	18725
20	5	3605	1.21	0.45	1.16	0.27	5117	1547
20	10	3605	0.68	0.20	1.07	0.21	1585	516
50	1	9041	70.69	31.89	9.11	2.66	175979	28195
50	5	9041	4.17	1.58	1.57	0.33	13737	2329
50	10	9041	1.57	0.54	1.15	0.21	3989	858
100	1	18086	280.22	100.87	25.45	9.66	390873	44162
100	5	18086	13.11	4.73	2.11	0.51	27920	3515
100	10	18086	3.80	1.35	1.32	0.34	8126	1419

458 Note that all reported instances were solved to optimality w.r.t. both maximum
459 energy functions. Using $E_v^{\text{max-lb}}$ as maximum energy function, the static approach as well
460 as the cutting plane approach were both able to solve all instances within few seconds.
461 However, the static approach is significantly faster than the cutting plane method for all
462 considered instance groups.

463 Using $E_v^{\text{max-ex}}$ as maximum energy function, though, the cutting plane method
464 shows its performance advantages with growing n . Due to how $E_v^{\text{max-lb}}$ and $E_v^{\text{max-ex}}$ are
465 derived, the number of piecewise linear segments for $E_v^{\text{max-ex}}$ is in general much higher
466 than for $E_v^{\text{max-lb}}$. As the number of segments increases we can observe that the cutting
467 plane approach scales significantly better than the static approach. This improvement
468 is particularly noticeable if we fix n and consider decreasing Δt values. Observe that,
469 for a fixed Δt the number of cuts increases with larger n values, whereas for a fixed n
470 the number of cuts increases with smaller Δt values. Therefore, the results indicate that
471 the cutting plane technique shows performance benefits when a larger number of cuts
472 has to be separated, i.e., the maximum charging power condition was not easily fulfilled.

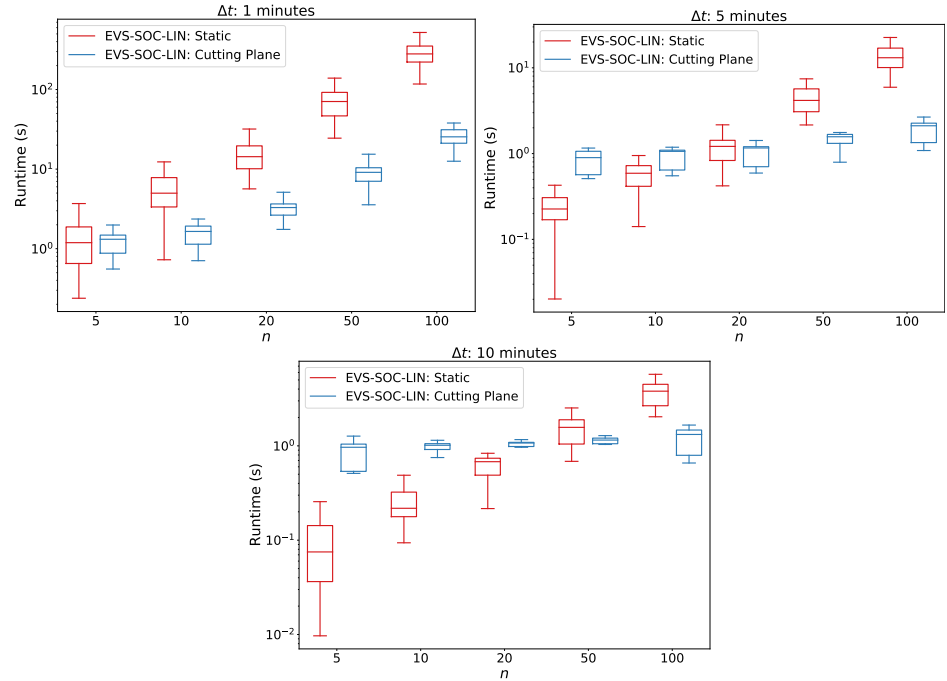


Figure 6. EVS-SOC-LIN runtime comparison for directly solving the LP problem versus the cutting plane approach, corresponding to results of Table 2.

473 Overall, it can be said that the cutting plane variant outperforms the static model on
 474 larger instances and when n_{seg} is large. We additionally conducted the experiments for
 475 $P_{\text{gridmax}} = 10n$ and $40n$ and observed the same trends.

476 In Figure 6 we give a more detailed comparison of the runtimes between the static
 477 approach and the cutting plane approach with $E_v^{\text{max-ex}}$ as maximum energy function.
 478 The figure shows that, when fixing Δt , the static approach does not scale as well as
 479 the cutting plane approach in terms of computation time with an increasing number of
 480 vehicles. For $\Delta t \in \{5, 10\}$ the runtimes of the cutting plane approach barely increase as
 481 n grows. Only for $\Delta t = 1$ minute the runtimes of the cutting plane approach increase
 482 slightly with a growing number of vehicles. In contrast, for the static approach the
 483 computation times increase much stronger than their cutting plane counterparts. As Δt
 484 decreases the difference in performance becomes more and more obvious.

485 6.2. EVS-SOC-GLIN

486 Similar to before, we compare two variants of EVS-SOC-GLIN for the general
 487 nonconcave maximum charging power functions. In the first variant we directly solve
 488 the static MILP in which all linking constraints (17–19) are included from the beginning,
 489 whereas the second approach is the branch-and-cut variant (B&C) in which these linking
 490 constraints are dynamically separated as needed, cf. Section 4.2. As maximum energy
 491 function we use $E_v^{\text{max-ex}}$ and $E_v^{\text{max-lb}}$, both based on the original full resolution P_v^{max}
 492 functions. For $P_{\text{gridmax}} \in \{10n, 25n, 40n\}$ we report the results in Tables 3, 4, and
 493 5, respectively. Columns, n_{seg} denote the total number of piecewise linear segments
 494 functions E_v^{max} consist of, summed over all n vehicles of an instance. Columns n_{feas}
 495 indicate the numbers of instances per group to which feasible solutions have been found
 496 and columns “Runtime” list the median computation times per group. Again, n_{cuts} refers
 497 to the total number of cuts added within B&C. The last columns indicate the finally
 498 remaining optimality gaps between lower and upper bounds as reported by Gurobi. These
 499 gaps are calculated as the absolute difference between the respective upper and lower
 500 bounds divided by the upper bound. Moreover, for visual representation of the number
 501 of feasibly solved instances, the median runtimes, and the number of added cuts within
 502 B&C see Figure 7–9. Only gaps of instances with a feasible solution are considered. For

parameter combinations without gaps (marked with “-”), no feasible solution has been found for any instance within the time limit. For parameter combinations where no runtime is reported, all corresponding runs terminated due to an out-of-memory error. More detailed results can be found in Appendix B where also the number of instances solved to optimality as well as standard deviations for runtimes and the numbers of cuts are reported.

Opposed to EVS-SOC-LIN, not all instances could be solved by the EVS-SOC-GLIN variants within the time limit. Considering the results with $P^{\text{gridmax}} = 10n$, one can notice that the B&C approach shows performance benefits, as the approach was able to always find feasible solutions to as many or more instances than the static approach. It is difficult to compare the quality of the solutions obtained by each approach as the static approach sometimes found fewer feasible solutions. For groups for which both approaches could obtain feasible solutions to all instances, the quality of the generated solutions is almost identical. Moreover, except for two instance groups, the B&C approach was either as fast or faster than the static approach.

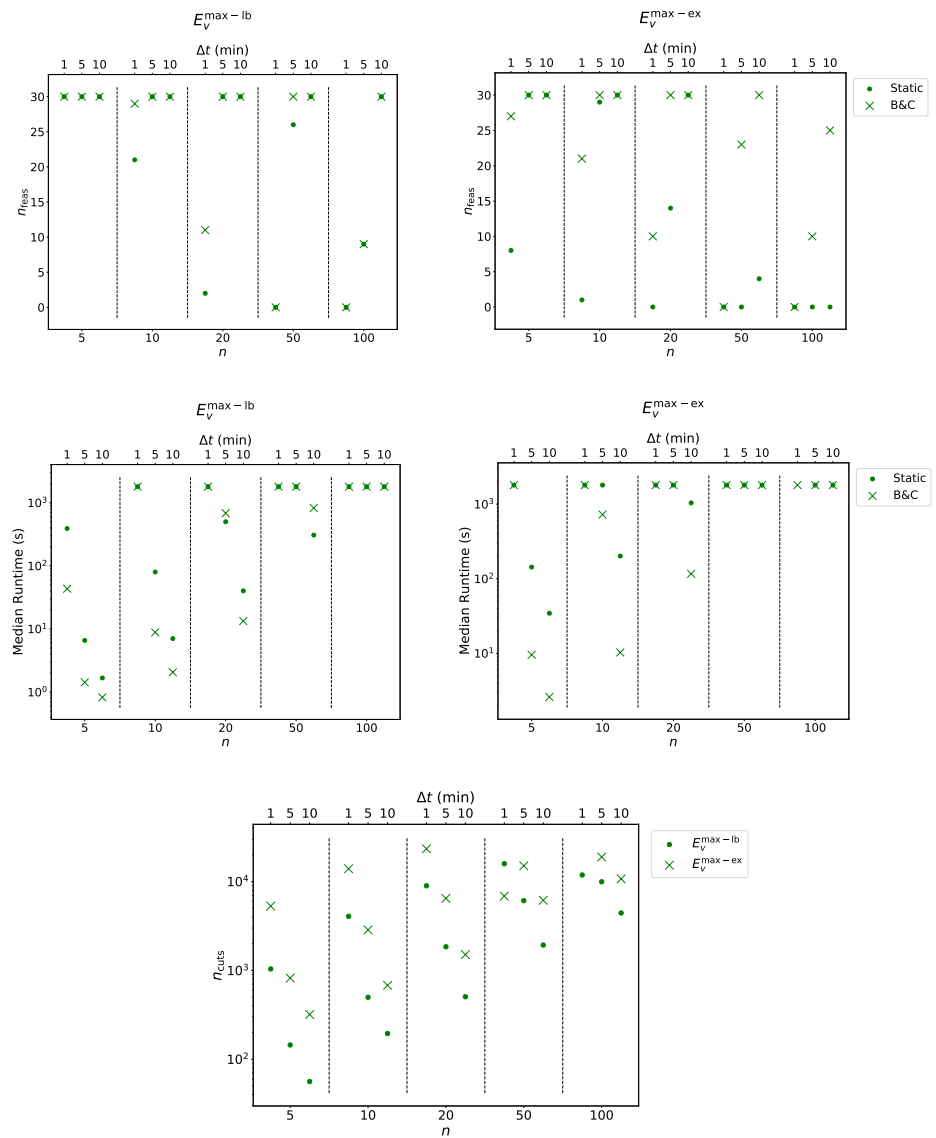


Figure 7. Visualization of EVS-SOC-GLIN results for solving the static model versus B&C with $E_v^{\text{max-lb}}$ based on five-segment piecewise linear approximations of the original P_v^{max} functions, $P^{\text{gridmax}} = 10n$.

Table 3: EVS-SOC-GLIN results for solving the static model versus B&C with $E_v^{\max\text{-lb}}$ and $E_v^{\max\text{-ex}}$ based on the original P_v^{\max} functions and $P_{\text{gridmax}} = 10n$.

n	Δt (min)	n_{seg}	n_{feas}		Runtime (s)		n_{cuts}	%gap		
		Mean	Static	B&C	Static	B&C	Median	Median	Static	B&C
$E_v^{\max\text{-lb}}$										
5	1	155	30	30	391.75	43.39	1038	0.01	0.01	
5	5	139	30	30	6.58	1.43	144	0.00	0.01	
5	10	119	30	30	1.67	0.83	56	0.00	0.00	
10	1	311	21	29	1800.00	1800.00	4068	0.03	0.03	
10	5	279	30	30	79.94	8.84	498	0.01	0.01	
10	10	242	30	30	7.04	2.06	194	0.00	0.01	
20	1	612	2	11	1800.00	1800.00	8974	0.08	0.19	
20	5	553	30	30	500.49	684.63	1846	0.01	0.01	
20	10	475	30	30	40.18	13.35	505	0.01	0.01	
50	1	1544	0	0	1800.00	1800.00	15910	-	-	
50	5	1393	26	30	1800.00	1800.00	6106	0.05	0.05	
50	10	1192	30	30	307.62	827.59	1930	0.01	0.01	
100	1	3095	0	0	1800.00	1800.00	11886	-	-	
100	5	2796	9	9	1800.00	1800.00	9961	0.08	0.12	
100	10	2399	30	30	1800.00	1800.00	4434	0.01	0.03	
$E_v^{\max\text{-ex}}$										
5	1	901	8	27	1800.00	1800.00	5304	0.03	0.01	
5	5	901	30	30	143.42	9.59	820	0.00	0.00	
5	10	901	30	30	34.53	2.60	319	0.00	0.00	
10	1	1802	1	21	1800.00	1800.00	13982	0.04	0.08	
10	5	1802	29	30	1800.00	725.37	2858	0.01	0.01	
10	10	1802	30	30	201.32	10.29	680	0.00	0.01	
20	1	3605	0	10	1800.00	1800.00	23449	-	0.14	
20	5	3605	14	30	1800.00	1800.00	6479	0.07	0.05	
20	10	3605	30	30	1038.91	116.59	1507	0.01	0.01	
50	1	9041	0	0	1800.00	1800.00	6856	-	-	
50	5	9041	0	23	1800.00	1800.00	15048	-	0.11	
50	10	9041	4	30	1800.00	1800.00	6160	0.18	0.03	
100	1	18078	0	0	-	1800.00	0	-	-	
100	5	18086	0	10	1800.00	1800.00	18944	-	0.08	
100	10	18086	0	25	1800.00	1800.00	10750	-	0.06	

518 For the results with $P_{\text{gridmax}} = 25n$, the runtime performance benefit of B&C is still
519 noticeable for small n , however it is not as strong as for $P_{\text{gridmax}} = 10n$. Moreover, for
520 $E_v^{\max\text{-lb}}$ the number of feasible solutions found by the static approach is, except for one
521 group, never worse than for B&C. Though, for $E_v^{\max\text{-ex}}$ B&C still yielded significantly
522 more feasible solutions.

523 A similar observation can be made for $P_{\text{gridmax}} = 40n$. For $P_{\text{gridmax}} = 40n$, the
524 static approach has a better runtime with almost all parameter configurations.

525 A possible explanation for this observation seems to be that for $P_{\text{gridmax}} = 10n$ the
526 charging energy of a vehicle v is more limited by P_{gridmax} than by E_v^{\max} . Initial solutions
527 of B&C will then violate Constraints (14) less often, which implies spending less time
528 for the separation of cuts. This presumption is supported by considering the number of
529 added cuts. Fixing n and Δt , one can observe that with growing P_{gridmax} clearly more
530 cuts are added.

531 When comparing $E_v^{\max\text{-lb}}$ and $E_v^{\max\text{-ex}}$ for any fixed P_{gridmax} , n , and Δt , $E_v^{\max\text{-ex}}$
532 has more segments than $E_v^{\max\text{-lb}}$ due to the nature of its computation. Also, for $E_v^{\max\text{-lb}}$
533 smaller Δt values imply a higher number of $E_v^{\max\text{-lb}}$ segments. For a fixed n and Δt
534 the larger number of $E_v^{\max\text{-ex}}$ segments comes with fewer feasible solutions and higher
535 runtimes for the static approach and the B&C.

Table 4: EVS-SOC-GLIN results for solving the static model versus B&C with $E_v^{\max\text{-lb}}$ and $E_v^{\max\text{-ex}}$ based on the original P_v^{\max} functions and $P^{\text{gridmax}} = 25n$.

n	Δt (min)	n_{seg}	n_{feas}		Runtime (s)		n_{cuts}	%gap		
		Mean			Median		Median	Median		
			Static	B&C	Static	B&C	B&C	Static	B&C	
$E_v^{\max\text{-lb}}$										
5	1	155	29	30	1800.00	1800.00	3184	0.02	0.06	
5	5	139	30	30	25.52	6.68	422	0.01	0.01	
5	10	119	30	30	1.27	1.62	153	0.01	0.01	
10	1	312	20	23	1800.00	1800.00	7298	0.10	0.12	
10	5	279	30	30	183.39	770.59	1132	0.01	0.01	
10	10	242	30	30	17.87	11.88	452	0.01	0.01	
20	1	612	4	3	1800.00	1800.00	11938	0.26	0.28	
20	5	553	30	30	1800.00	1800.00	2702	0.01	0.05	
20	10	475	30	30	60.59	201.06	967	0.01	0.01	
50	1	1544	0	0	1800.00	1800.00	22034	-	-	
50	5	1393	29	30	1800.00	1800.00	6997	0.08	0.11	
50	10	1192	30	30	902.21	1800.00	2575	0.01	0.03	
100	1	3095	0	0	1800.00	1800.00	29193	-	-	
100	5	2796	14	7	1800.00	1800.00	11737	0.12	0.18	
100	10	2399	30	30	1800.00	1800.00	5340	0.03	0.06	
$E_v^{\max\text{-ex}}$										
5	1	901	9	25	1800.00	1800.00	15258	0.21	0.20	
5	5	901	30	30	448.47	761.59	2153	0.01	0.01	
5	10	901	30	30	56.12	16.43	866	0.00	0.01	
10	1	1802	1	18	1800.00	1800.00	23328	0.23	0.33	
10	5	1802	26	30	1800.00	1800.00	5220	0.04	0.06	
10	10	1802	30	30	204.26	233.60	2063	0.01	0.01	
20	1	3605	0	2	1800.00	1800.00	17970	-	0.32	
20	5	3605	15	29	1800.00	1800.00	10784	0.08	0.12	
20	10	3605	29	30	1097.26	1800.00	4647	0.01	0.03	
50	1	9041	0	0	1800.00	1800.00	23986	-	-	
50	5	9041	0	17	1800.00	1800.00	23708	-	0.18	
50	10	9041	16	28	1800.00	1800.00	12160	0.04	0.08	
100	1	18086	0	0	1800.00	1800.00	0	-	-	
100	5	18086	0	0	1800.00	1800.00	25754	-	-	
100	10	18086	0	19	1800.00	1800.00	19752	-	0.09	

536 In general, regardless of P^{gridmax} , all reported median gaps for both approaches are
537 below 0.2%. Moreover, while the B&C approach usually finds a higher number of feasible
538 solutions, the static approach finds generally more optimal solutions, as can be seen in
539 Appendix B.

540 In order to see how both solution approaches to EVS-SOC-GLIN perform on instances
541 with fewer piecewise linear segments in E_v^{\max} , we conduct similar experiments using the
542 approximations of P_v^{\max} with five segments. For this we only consider $E_v^{\max\text{-lb}}$, since
543 the number of $E_v^{\max\text{-ex}}$ segments does not depend on the number of P_v^{\max} segments.
544 Experimental results for $P^{\text{gridmax}} = 25n$ are given in Table 6. The table shows again the
545 total number of piecewise linear segments of $E_v^{\max\text{-lb}}$ (n_{seg}), the number of instances for
546 which a feasible solutions was found within the time limit (n_{feas}), the median computation
547 time (“Runtime”), the total number of cuts added within B&C (n_{cuts}), and optimality
548 gaps (%-gap) of the generated solutions.

549 For each parameter group, B&C always finds at least as many feasible solutions as
550 the static approach. When the static and the B&C approaches find the same number of
551 feasible solutions, the resulting gaps are almost identical, though, the solutions of the
552 static variant are typically slightly better than the ones of B&C. In terms of computation
553 times, no approach is significantly faster than the other.

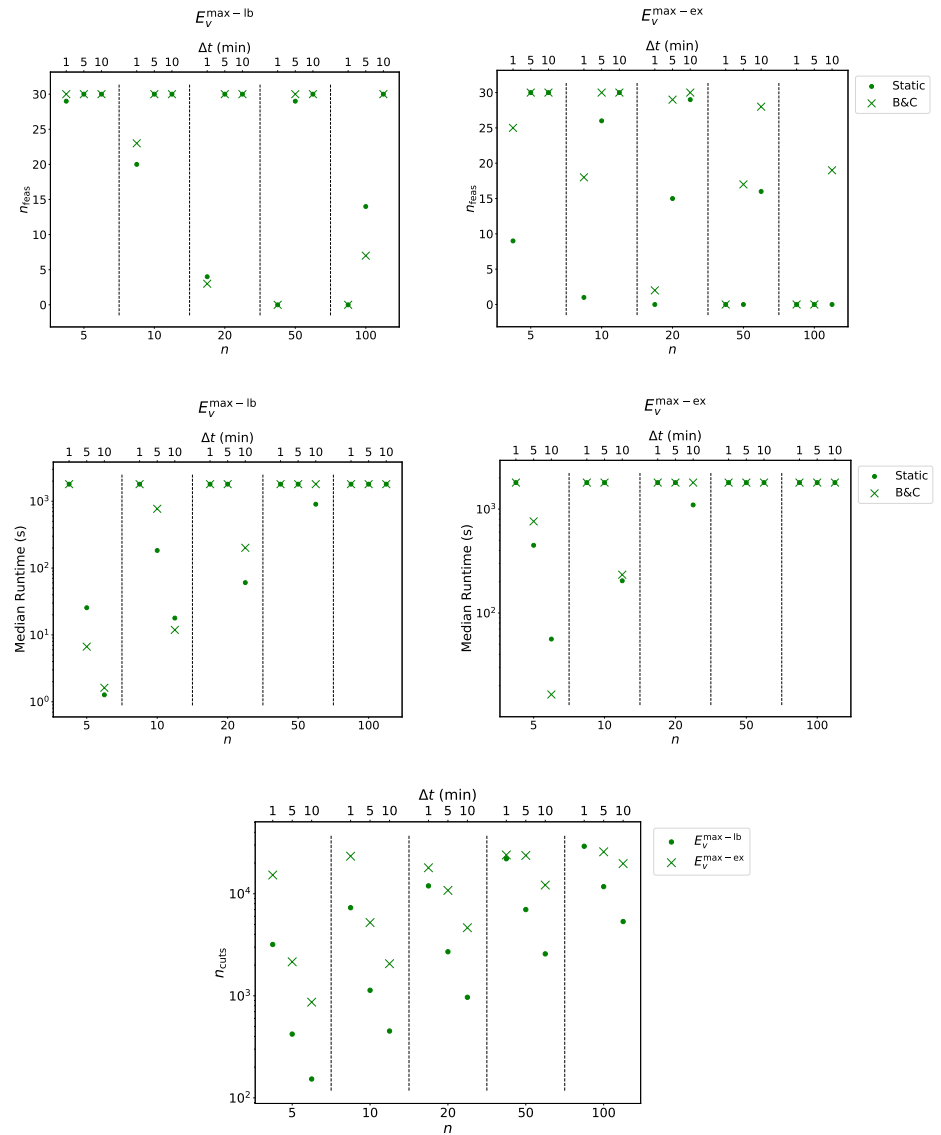


Figure 8. Visualization of EVS-SOC-GLIN results for solving the static model versus B&C with $E_v^{\max-lb}$ based on five-segment piecewise linear approximations of the original P_v^{\max} functions, $p_{gridmax} = 25n$.

554 Due to the smaller number of segments in the P_v^{\max} functions and consequently also
 555 simpler $E_v^{\max-lb}$ functions, a higher number of feasible as well as optimal solutions could
 556 generally be found, when comparing Tables 6 and 4. Moreover, the impact of fewer P_v^{\max}
 557 segments is also observable when we consider the median runtimes and the number of
 558 added cuts. For almost all parameter combinations of n and Δt , fewer P_v^{\max} segments
 559 lead to lower median runtimes and fewer cuts.

560 6.2.1. Charging Cost Differences & Charging Errors

561 While the simpler approximations of the original P_v^{\max} functions lead to shorter
 562 runtimes, there is clearly a tradeoff concerning the precision of the model, introduced
 563 errors, and final solution qualities. We have a closer look on these aspects in the following.
 564 Specifically, we are interested in the error made when using $E_v^{\max-lb}$ instead of $E_v^{\max-ex}$ and
 565 the error between the five-segment P_v^{\max} approximation compared to the original P_v^{\max} .
 566 For this purpose, we evaluate EVS-SOC-GLIN on four different E_v^{\max} functions: $E_v^{\max-lb}$
 567 and $E_v^{\max-ex}$, each based on the five-segment P_v^{\max} approximation and the original P_v^{\max} .

Table 5: EVS-SOC-GLIN results for solving the static model versus B&C with $E_v^{\max\text{-lb}}$ and $E_v^{\max\text{-ex}}$ based on the original P_v^{\max} functions and $P^{\text{gridmax}} = 40n$.

n	Δt (min)	n_{seg}	n_{feas}		Runtime (s)		n_{cuts}	%gap		
		Mean	Static	B&C	Static	B&C	Median	Median	Static	B&C
$E_v^{\max\text{-lb}}$										
5	1	155	29	29	1800.00	1800.00	4476	0.04	0.15	
5	5	139	30	30	31.04	55.93	619	0.01	0.01	
5	10	119	30	30	2.49	4.05	247	0.01	0.01	
10	1	311	20	20	1800.00	1800.00	8161	0.21	0.17	
10	5	279	30	30	301.14	1800.00	1410	0.01	0.03	
10	10	242	30	30	27.80	36.06	456	0.01	0.01	
20	1	612	2	1	1800.00	1800.00	13361	0.27	0.48	
20	5	553	30	30	1800.00	1800.00	2863	0.04	0.10	
20	10	475	30	30	69.51	571.16	1078	0.01	0.01	
50	1	1544	0	0	1800.00	1800.00	25908	-	-	
50	5	1393	28	28	1800.00	1800.00	7110	0.12	0.21	
50	10	1192	30	30	1097.80	1800.00	2748	0.01	0.05	
100	1	3095	0	0	1800.00	1800.00	29066	-	-	
100	5	2796	7	2	1800.00	1800.00	11782	0.22	0.21	
100	10	2399	29	30	1800.00	1800.00	5650	0.06	0.10	
$E_v^{\max\text{-ex}}$										
5	1	901	9	24	1800.00	1800.00	20190	0.23	0.44	
5	5	901	30	30	582.18	1800.00	3180	0.01	0.07	
5	10	901	30	30	80.12	34.07	1228	0.00	0.01	
10	1	1802	1	13	1800.00	1800.00	24450	0.49	0.77	
10	5	1802	26	30	1800.00	1800.00	6026	0.02	0.17	
10	10	1802	30	30	245.17	1147.26	2161	0.01	0.01	
20	1	3605	0	0	1800.00	1800.00	17460	-	-	
20	5	3605	15	29	1800.00	1800.00	13276	0.14	0.22	
20	10	3605	29	30	1437.18	1800.00	5692	0.01	0.08	
50	1	9041	0	0	1800.00	1800.00	12253	-	-	
50	5	9041	0	11	1800.00	1800.00	27617	-	0.21	
50	10	9041	14	27	1800.00	1800.00	13538	0.10	0.12	
100	1	18083	0	0	-	1800.00	0	-	-	
100	5	18086	0	0	1800.00	1800.00	31692	-	-	
100	10	18086	0	11	1800.00	1800.00	23081	-	0.14	

568 Since we want to measure the impact of the different charging curves on the charging
569 costs, we select a high P^{gridmax} value of $40n$ as in this case the variable maximum charging
570 power constraints have higher impact. Only results on instances solved to optimality
571 are reported. Also, we only consider instances where an optimal solution for all four
572 E_v^{\max} functions was found. Parameter combinations where no such instances exist are
573 omitted. The mean charging costs can be found in Table 7. The charging cost %-gaps
574 are calculated by $100\% \cdot (|E_v^{\max\text{-ex}} - E_v^{\max\text{-lb}}|) / E_v^{\max\text{-ex}}$.

575 Observe that for fixed Δt and varying n , the charging cost gap between $E_v^{\max\text{-lb}}$ and
576 $E_v^{\max\text{-ex}}$ does not change significantly. It seems that the difference in charging costs mainly
577 depends on Δt . Specifically, one might notice that the charging cost gaps become smaller
578 as Δt decreases. Overall, the largest mean charging cost gap is 0.64%, the differences
579 therefore seem to be negligible for practical purposes for the considered parameter groups.
580 Note however that not all instances could be solved to optimality (even when increasing
581 the time limit) and hence the number of reported instances in some instance groups
582 varies for each instance group. Therefore, to give a better idea about the distribution
583 of the charging cost gaps, we additionally provide standard deviations to the charging
584 cost gaps in Table 7. For groups with the same Δt we can observe that the standard
585 deviations are quite similar.

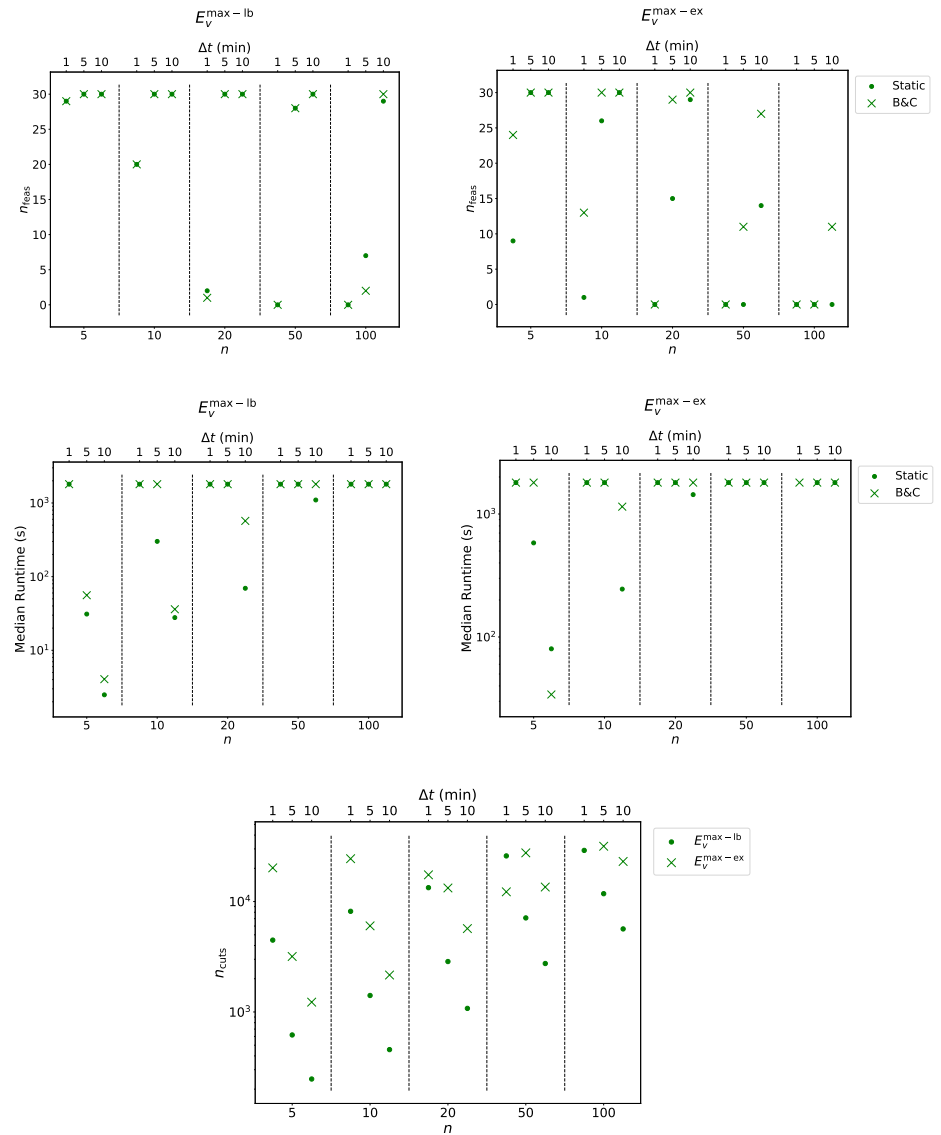


Figure 9. Visualization of EVS-SOC-GLIN results for solving the static model versus B&C with $E_v^{\max-lb}$ based on five-segment piecewise linear approximations of the original P_v^{\max} functions, $P_{gridmax} = 40n$.

586 When comparing the five-segment P_v^{\max} approximation to the original P_v^{\max} , the
 587 difference in charging costs is marginal, even for large instances. For example consider
 588 $n = 20$, $\Delta t = 10$ minutes and $E_v^{\max-ex}$ and observe that the objective value differs
 589 on average by about 0.07 cent only between the original P_v^{\max} and the five-segment
 590 approximation. This insight seems to be particularly relevant, since it shows that
 591 approximating P_v^{\max} with a lower number of linear pieces is reasonable for practice.

592 When realizing a charging plan in practice with a different E_v^{\max} function than used
 593 for scheduling, the specified target SOC's s_v^{dep} might not be reached for some vehicles.
 594 We measure this error by generating an *optimal* charging schedule with $E_v^{\max-ex}$ and
 595 simulating the actual maximum energy function with $E_v^{\max-lb}$. In the simulation, the
 596 actually charged energy is set to the minimum from the corresponding planned charged
 597 energy and the actual maximum energy function. The resulting mean deviation from
 598 the target SOC in percent, the mean charging error, can be seen in Table 8. For a single
 599 instance, we determined the mean charging error over all vehicles, whereas for an instance
 600 group we again report the mean and the standard deviation of these mean charging errors
 601 from the individual instances.

Table 6: EVS-SOC-GLIN results for solving the static model versus B&C with $E_v^{\max\text{-lb}}$ based on five-segment piecewise linear approximations of the original P_v^{\max} functions, $P_{\text{gridmax}} = 25n$.

n	Δt (min)	n_{seg}	n_{feas}		Runtime (s)		n_{cuts}	%gap		
		Mean	Static	B&C	Median		Median	Median		
					Static	B&C		Static	B&C	
$E_v^{\max\text{-lb}}$										
5	1	40	30	30	60.14	19.63	387	0.01	0.01	
5	5	46	30	30	2.40	1.98	88	0.01	0.01	
5	10	43	30	30	0.64	1.13	42	0.00	0.01	
10	1	80	30	30	509.28	1800.00	1162	0.01	0.02	
10	5	92	30	30	11.01	8.34	232	0.01	0.01	
10	10	87	30	30	1.49	2.68	118	0.01	0.01	
20	1	160	12	30	1800.00	1800.00	2488	0.03	0.06	
20	5	185	30	30	54.58	61.09	516	0.01	0.01	
20	10	174	30	30	5.03	7.45	217	0.01	0.01	
50	1	398	0	12	1800.00	1800.00	5598	-	0.24	
50	5	459	30	30	640.74	1800.00	1556	0.01	0.02	
50	10	433	30	30	37.23	36.95	624	0.01	0.01	
100	1	798	0	0	1800.00	1800.00	9312	-	-	
100	5	921	30	30	1800.00	1800.00	3237	0.01	0.06	
100	10	871	30	30	112.16	84.83	1360	0.01	0.01	

Table 7: Objective value comparison using EVS-SOC-GLIN and different E_v^{\max} functions based on the five-segment P_v^{\max} approximation and the original P_v^{\max} ; $P_{\text{gridmax}} = 40n$.

n	Δt (min)	n_{opt}	Charging Costs			
			$E_v^{\max\text{-lb}}$	$E_v^{\max\text{-ex}}$	%gap	
			Mean	Mean	Mean	StdDev
Original P_v^{\max}						
5	1	2	109.08	108.97	0.10	0.01
5	5	25	209.40	208.83	0.29	0.18
5	10	30	227.10	225.78	0.64	0.40
10	5	11	374.24	372.98	0.34	0.13
10	10	28	447.51	445.05	0.59	0.35
20	10	19	882.53	877.33	0.60	0.30
5-segment approx. P_v^{\max}						
5	1	2	109.10	108.98	0.10	0.01
5	5	25	209.38	208.82	0.29	0.17
5	10	30	227.11	225.77	0.64	0.41
10	5	11	374.14	372.92	0.33	0.13
10	10	28	447.44	445.04	0.57	0.32
20	10	19	882.39	877.26	0.60	0.30

602 Similarly to before, it seems that the size of the charging error mainly depends on Δt :
603 Fixing the number of vehicles n , the mean charging error decreases with smaller Δt , the
604 number of vehicles does not seem to influence the mean charging error for fixed Δt .

605 6.3. Comparison of EVS-SOC-LIN and EVS-SOC-GLIN

606 Charging cost gaps between solutions of formulation EVS-SOC-LIN and EVS-SOC-
607 GLIN can be found in Figure 10. As before, we only consider instances that were
608 solved to optimality. For EVS-SOC-LIN we use $E_v^{\max\text{-lb}}$ based on the concave P_v^{\max} ,
609 whereas for EVS-SOC-GLIN we use $E_v^{\max\text{-lb}}$ based on P_v^{\max} with five segments. The grid
610 capacity P_{gridmax} is again set to $40n$. Charging cost gaps are calculated by dividing the
611 difference of the EVS-SOC-GLIN objective values from the EVS-SOC-LIN objectives by
612 the EVS-SOC-GLIN objective values. For $n \in \{50, 100\}$ and $\Delta t = 1$ minute, all mean
613 charging cost gaps are zero, therefore the respective bars are not shown in the figure.

Table 8: Charging error comparison when scheduling with $E_v^{\max\text{-ex}}$ using EVS-SOC-GLIN and realizing the schedule with $E_v^{\max\text{-lb}}$; $P_{\text{gridmax}} = 40n$.

n	Δt (min)	n_{opt}	Mean Charging Error (% SOC)			
			Original P_v^{\max}		5-seg. approx. P_v^{\max}	
			Mean	StdDev	Mean	StdDev
5	1	3	0.23	0.08	0.21	0.08
5	5	25	1.14	0.26	1.06	0.28
5	10	30	2.01	0.58	1.94	0.60
10	5	12	1.14	0.16	1.18	0.18
10	10	29	2.03	0.45	2.03	0.46
20	10	20	2.01	0.29	1.97	0.34

614 Comparing the gaps of both formulations, one can notice that the charging costs of
 615 solutions generated by EVS-SOC-LIN are slightly too optimistic, underestimating the
 616 actual costs. In comparison to the more exact EVS-SOC-GLIN, the costs of the solutions
 617 generated by EVS-SOC-LIN are lower by at most by 0.35%. Moreover, there are no
 618 significant differences between the charging cost gaps when varying n or Δt values. When
 619 it comes to computation times, both variants of EVS-SOC-LIN are significantly faster
 620 than any EVS-SOC-GLIN variant, as we have seen before in Table 2 and Table 4.

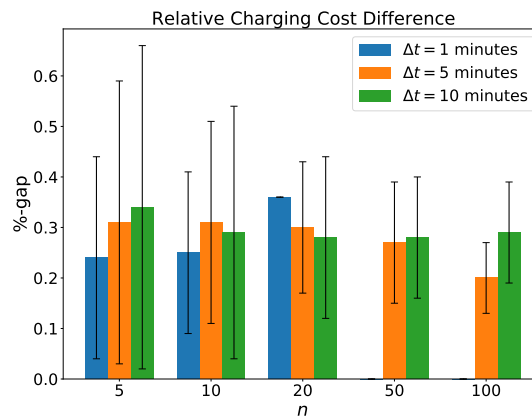


Figure 10. Mean charging cost gaps of EVS-SOC-LIN and EVS-SOC-GLIN with $P_{\text{gridmax}} = 40n$. Whiskers indicate the standard deviations. Note that for $n = 20$ and $\Delta t = 1$ only a single instance was solved to optimality and therefore the corresponding standard deviation is zero.

621 For the exact same setting as above, we also measure the charging error when
 622 scheduling with the convex $E_v^{\max\text{-lb}}$ used in EVS-SOC-LIN and realizing the plan with
 623 the, in general, nonconvex $E_v^{\max\text{-lb}}$ used in EVS-SOC-GLIN. The mean charging error
 624 is shown in Figure 11. It can be said that for a fixed Δt , the mean charging error does
 625 not significantly change for a varying number of vehicles n . However, for a fixed number
 626 n , the mean charging error grows with decreasing Δt . An explanation for this behavior
 627 seems to be that on instances with smaller Δt , solutions tend to be more precise in terms
 628 of the error induced by the time discretization. Therefore the difference between a convex
 629 and nonconvex E_v^{\max} function could have more impact on solutions of instances with
 630 small Δt values. Overall, the mean charging cost difference does not exceed 1.5% SOC
 631 for any n and any Δt and, thus, may be negligible in practice.

632 6.4. Model Based Predictive Control Simulations

633 For the rolling horizon scenarios, we conduct experiments using formulations EVS-
 634 SOC-LIN and EVS-SOC-GLIN. We use $E_v^{\max\text{-lb}}$ for both formulations, but for EVS-SOC-
 635 LIN the corresponding concave approximation of P_v^{\max} , whereas for EVS-SOC-GLIN the
 636 five-segment approximation of P_v^{\max} . P_{gridmax} is set to $40n$. Results of the experiments
 637 are shown in Table 9. Absolute charging cost differences are determined by subtracting

638 the EVS-SOC-GLIN objective values from the EVS-SOC-LIN objective values. Relative
 639 charging costs are based on the absolute charging costs divided by the objective values of
 640 EVS-SOC-GLIN.

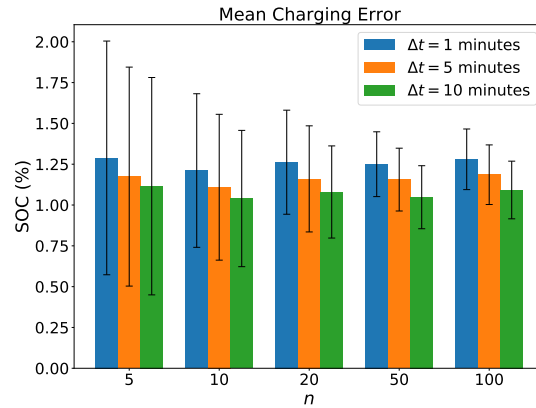


Figure 11. Mean charging error when scheduling with convex $E_v^{\max\text{-lb}}$ and realizing the plan with nonconvex $E_v^{\max\text{-lb}}$ using $P^{\text{gridmax}} = 40n$. Whiskers indicate the standard deviations.

641 Similarly to before, for fixed n and Δt , the charging costs of EVS-SOC-LIN and
 642 EVS-SOC-GLIN only differ marginally. The maximum gap is 0.27% for $n = 100$ and
 643 $\Delta t = 5$ minutes. As expected, the absolute charging cost difference increases with a higher
 644 number of vehicles. The gaps, however, seem to stay in the same order of magnitude for
 645 growing n .

Table 9: Rolling horizon charging cost difference for EVS-SOC-LIN vs. EVS-SOC-GLIN using $E_v^{\max\text{-lb}}$; $P^{\text{gridmax}} = 40n$.

n	Δt (min)	Charging Cost Difference			
		Absolute (cent)		Relative (%)	
		Mean	StdDev	Mean	StdDev
5	5	0.97	0.73	0.22	0.16
5	10	0.91	0.60	0.20	0.12
10	5	1.75	0.99	0.20	0.11
10	10	1.78	0.77	0.20	0.08
20	5	3.78	1.34	0.21	0.08
20	10	3.80	1.03	0.21	0.06
50	5	9.14	2.42	0.20	0.05
50	10	9.39	2.64	0.21	0.06
100	5	24.42	2.40	0.27	0.03
100	10	19.96	4.82	0.22	0.05

646 7. Conclusions

647 We formally introduced the EVS-SOC problem in which we put particular focus on
 648 dealing with vehicle-specific SOC-dependent maximum charging power limitations. We
 649 addressed the issue that the maximum charging power P_v^{\max} may be regulated within a
 650 single time step in a time discretized solution approach by turning towards considering
 651 the maximum amount of energy that can be charged in a time step. To this end, we
 652 proposed an exact derivation $E_v^{\max\text{-ex}}$ as well as a simpler lower bound $E_v^{\max\text{-lb}}$. One
 653 should keep in mind that the gap between $E_v^{\max\text{-lb}}$ and $E_v^{\max\text{-ex}}$ decreases with smaller
 654 time step duration Δt . We recall that charging schedules generated with $E_v^{\max\text{-lb}}$ are
 655 guaranteed to be realizable in practice, whereas schedules generated with $E_v^{\max\text{-ex}}$ help
 656 us with the estimation of the charging cost differences and charging errors induced by
 657 the time discretization.

658 Let us recapitulate the most important experimental results. Two different MILP
 659 formulations, EVS-SOC-LIN and EVS-SOC-GLIN, were proposed, where EVS-SOC-LIN
 660 relies on the assumption that E_v^{\max} is concave. When taking a closer look at EVS-SOC-
 661 LIN, both the static as well as the cutting plane variant, are quite fast. Compared to
 662 EVS-SOC-GLIN, EVS-SOC-LIN performs an order of magnitude faster in our experiments.
 663 Considering the runtime difference between the static and the cutting plane approach,
 664 a substantial performance benefit of the latter can be observed. Moreover, we have
 665 seen that the runtime of the cutting plane approach scales better with larger numbers
 666 of vehicles or decreasing Δt values. Its advantages become even more visible when the
 667 maximum charging energy of a vehicle has to be exploited, i.e., a large number of cuts
 668 has to be separated.

669 Concerning the static solution approach and the B&C for solving EVS-SOC-GLIN,
 670 we found that B&C performs better for instances with a small number of vehicles. For
 671 larger instances, however, the static variant is usually superior in terms of runtime. It
 672 also shows performance advantages for larger grid capacities. Results of the experiments
 673 indicate that the B&C is slower than the static variant when a large number of cuts has
 674 to be separated. Nevertheless, there are cases where B&C is faster, for example when
 675 E_v^{\max} consists of many linear segments. Additionally, we realized that B&C finds more
 676 feasible solutions in the majority of the experiments, when solving to optimality is not
 677 possible anymore within the runtime limit. Overall, for both EVS-SOC-GLIN solution
 678 approaches it is also worth mentioning that fewer P_v^{\max} segments usually clearly reduce
 679 the runtime.

680 Different approximations of the maximum charging power (e.g., piecewise linear
 681 approximation or convex hull approximation), as well as the maximum charging energy
 682 ($E_v^{\max\text{-lb}}$, $E_v^{\max\text{-ex}}$) have been proposed. We studied the charging cost differences and the
 683 charging errors induced by these approximations. Regarding the charging cost differences,
 684 it turned out that there are only marginal charging cost differences between schedules
 685 generated with $E_v^{\max\text{-lb}}$ and schedules generated with $E_v^{\max\text{-ex}}$. The number of vehicles
 686 did not show any noticeable impact on the cost differences for this comparison. Naturally,
 687 a smaller step duration Δt reduces the charging cost differences. Moreover, in case of our
 688 benchmark instances the approximation of P_v^{\max} with five piecewise linear segments does
 689 not have any noticeable impact on the charging costs, despite the rather complex original
 690 functions. We also inspected the charging cost differences when generating schedules
 691 based on the original P_v^{\max} function and its concave approximation. It turned out that
 692 the charging cost differences are quite small, the mean differences did not exceed 0.35%
 693 for any shown parameter group.

694 As already mentioned, approximating the maximum charging energy might lead to
 695 the issue that vehicles do not reach their desired target SOC. To measure this effect,
 696 we generated charging schedules with $E_v^{\max\text{-ex}}$ and simulated the actual charging with
 697 $E_v^{\max\text{-lb}}$. Experimental results have shown that the mean charging error does not exceed
 698 2.1% SOC even for $\Delta t = 10$ minutes. For this experiments, we could also detect a
 699 correlation between the size of Δt and the charging error, more specifically the mean
 700 charging error decreases with smaller Δt . In another simulation, we considered the
 701 mean charging error when generating a charging schedule based on a concave P_v^{\max}
 702 approximation and realizing it with the original P_v^{\max} . The mean charging error is rather
 703 small again, the mean deviation from the vehicles' target SOC were at most 1.5%.

704 To see whether the concave approximation of P_v^{\max} accumulates large charging
 705 cost differences in a whole day scenario, we conducted model based predictive control
 706 simulations with the original P_v^{\max} and its concave approximation. The relative charging
 707 cost gaps were even smaller with a maximum value 0.27% for 100 vehicles and $\Delta t = 5$
 708 minutes.

709 Overall, where we utilize one of the formulations within a model based predictive
 710 control strategy, we recommend the usage of EVS-SOC-LIN or EVS-SOC-GLIN together
 711 with a reasonably small Δt value of few minutes, in order to reduce errors introduced by

712 time discretization. Depending on whether EVS-SOC-GLIN is performant enough for
713 a given application setting (i.e., it finds a charging schedule within the re-optimization
714 interval) its usage is advised to reduce the danger of significant charging cost differences
715 and charging errors. It seems promising to approximate P_v^{\max} with five to ten piecewise
716 linear segments to improve runtime in this scenario.

717 In case EVS-SOC-GLIN does not find charging schedules in reasonable time, one
718 might fall back to EVS-SOC-LIN and its cutting plane approach to rapidly generate
719 charging schedules for a concave approximation of P_v^{\max} . The introduced errors are
720 usually negligible as we have seen.

721 In future work it would be interesting to investigate whether the runtime of solving
722 EVS-SOC-GLIN can be further improved. As we have seen, B&C is frequently slower than
723 the static variant. A more detailed polyhedral study of the model may reveal additional
724 strengthening inequalities. Concerning the computational complexity of EVS-SOC, it is
725 an open question whether or not the problem is NP-hard if P_v^{\max} is a general nonconcave
726 function. Another aspect worth pursuing is the question whether known vehicle arrival
727 times have a significant impact on the charging costs of a rolling horizon schedule. In
728 the presented scenario, successively arriving vehicles are simulated, however they are not
729 incorporated into the schedule before arrival at the charging station. One may expect
730 that arrival times known in advance lead to better exploitation of cheap charging time
731 slots and therefore come along with cheaper total charging costs.

732 A further direction of future work should be the consideration of uncertainties, e.g.,
733 in the future power limits or in the future occupation of charging stations. Furthermore it
734 would be interesting to study the effect of the rescheduling interval on charging costs and
735 charging errors in the rolling horizon context. Last but not least, it would be interesting
736 to consider a problem variant in which discharging of vehicles is allowed in order to
737 enable mutual charging of EVs. This idea has already been mentioned in [27], however
738 its impact on the total charging costs has not yet been studied. One could further extend
739 the model by allowing the charging station to supply energy to the electricity grid in
740 exchange for monetary reward.

741 **Author Contributions:** Conceptualization, S.L., G.R.R.; methodology, S.L., G.R.R., and
742 B.S.; software, validation, B.S.; writing—original draft preparation, G.R.R, B.S., and T.J.;
743 writing—review and editing, S.L., G.R.R., B.S., and T.J.; supervision, S.L., G.R.R., and T.J.
744 All authors have read and agreed to the published version of the manuscript.

745 **Funding:** This research received no external funding

746 **Institutional Review Board Statement:** Not applicable.

747 **Informed Consent Statement:** Not applicable.

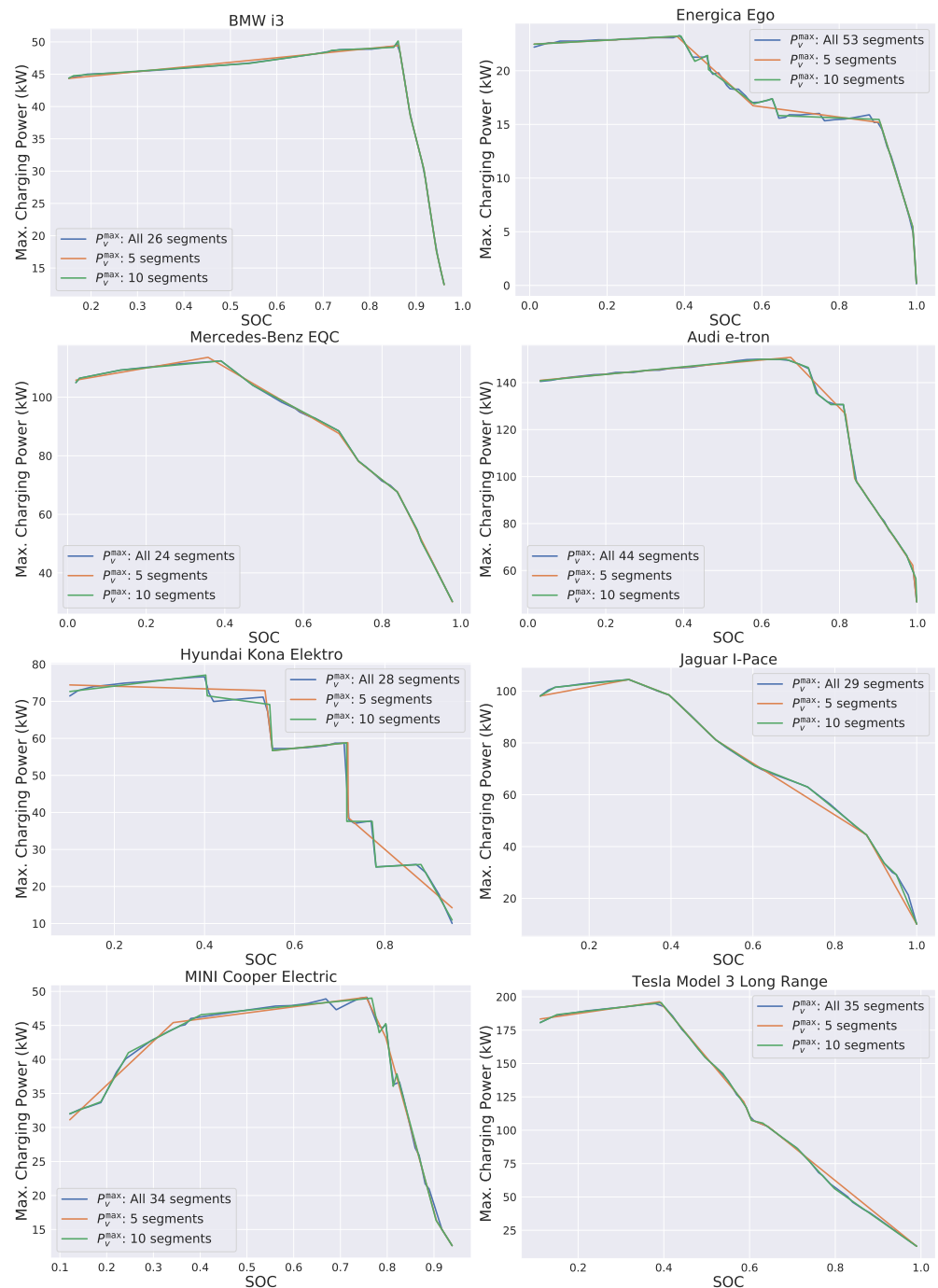
748 **Data Availability Statement:** All used benchmark problem instances are available at
749 <https://www.ac.tuwien.ac.at/research/problem-instances/>.

750 **Acknowledgments:** The project was financially supported by Honda Research Institute Europe
751 GmbH.

752 **Conflicts of Interest:** The authors declare no conflict of interest.

753 **Appendix A**

754 In Figure A1 a comparison between the original P_v^{\max} and the simpler piecewise approximations is shown for all vehicle types used in the benchmark instances.



755 **Figure A1.** Comparison of P_v^{\max} curves with different numbers of segments.

756 **Appendix B**

757 Tables 10, 11, 12, and 13 give more detailed information to the results provided in
 758 Tables 3, 4, 5, and 6, respectively. Shown here are also the numbers of optimally solved
 759 instances in each instance groups as well as standard deviations to the runtimes and the
 760 numbers of cuts.

Table 10: EVS-SOC-GLIN results for solving the static model versus B&C with $E_v^{\text{max-lb}}$ and $E_v^{\text{max-ex}}$ based on the original P_v^{max} functions and $P_{\text{gridmax}} = 10n$.

n	Δt (min)	n_{seg}		n_{opt}		n_{feas}		Runtime (s)				n_{cuts}		%gap		
		Mean	Static	B&C	Static	B&C	Static	B&C	Median	StdDev	Static	B&C	Median	StdDev	Static	B&C
$E_v^{\text{max-lb}}$																
5	1	155	24	24	30	30	30	391.75	43.39	662.53	720.28	1038	1944	0.01	0.01	
5	5	139	30	30	30	30	30	6.58	1.43	17.30	64.96	144	307	0.00	0.01	
5	10	119	30	30	30	30	30	1.67	0.83	6.66	1.77	56	120	0.00	0.00	
10	1	311	5	12	21	29	1800.00	1800.00	1800.00	389.82	764.87	4068	2726	0.03	0.03	
10	5	279	29	27	30	30	79.94	8.84	353.48	544.47	498	581	167	0.01	0.01	
10	10	242	30	30	30	30	7.04	2.06	35.58	4.31	8974	1820	0.08	0.19		
20	1	612	0	1	2	11	1800.00	1800.00	0.00	181.68	781.48	1846	1081	0.01	0.01	
20	5	553	23	19	30	30	500.49	684.63	640.95	781.48	425.71	505	274	0.01	0.01	
20	10	475	30	29	30	30	40.18	13.35	71.71	425.71	15910	2518	-	-		
50	1	1544	0	0	0	0	1800.00	1800.00	0.00	0.00	351.60	6106	1249	0.05	0.05	
50	5	1393	2	2	26	30	1800.00	1800.00	174.76	458.49	779.32	1930	594	0.01	0.01	
50	10	1192	29	18	30	30	307.62	827.59	0.00	0.00	11886	3940	-	-		
100	1	3095	0	0	0	0	1800.00	1800.00	0.00	0.00	9961	1319	0.08	0.12		
100	5	2796	0	0	9	9	1800.00	1800.00	0.00	0.00	4434	861	0.01	0.03		
100	10	2399	11	4	30	30	1800.00	1800.00	418.13	452.22	6069	6069	0.03	0.01		
$E_v^{\text{max-ex}}$																
5	1	901	3	12	8	27	1800.00	1800.00	414.46	834.31	628.62	5304	6069	0.00	0.00	
5	5	901	30	26	30	30	143.42	9.59	312.39	628.62	48.02	820	1553	0.00	0.00	
5	10	901	30	30	30	30	34.53	2.60	106.85	48.02	13982	7431	623	0.00	0.00	
10	1	1802	0	3	1	21	1800.00	1800.00	0.00	401.91	872.54	2858	2600	0.01	0.01	
10	5	1802	13	16	29	30	1800.00	725.37	568.29	872.54	680	845	0.00	0.01		
10	10	1802	30	28	30	30	201.32	10.29	327.78	451.48	23449	6856	-	0.14		
20	1	3605	0	0	0	10	1800.00	1800.00	0.00	0.00	6479	4009	0.07	0.05		
20	5	3605	2	6	14	30	1800.00	1800.00	85.05	629.36	862.58	1507	1708	0.01	0.01	
20	10	3605	22	18	30	30	1038.91	116.59	569.76	862.58	6856	4528	-	-		
50	1	9041	0	0	0	0	1800.00	1800.00	0.00	0.00	15048	3971	-	0.11		
50	5	9041	0	1	0	23	1800.00	1800.00	0.00	308.85	585.67	6160	3202	0.18	0.03	
50	10	9041	1	7	4	30	1800.00	1800.00	123.65	585.67	0.00	0	5698	-	-	
100	1	18078	0	0	0	0	-	1800.00	-	0.00	0.00	18944	5630	-	0.08	
100	5	18086	0	0	0	10	1800.00	1800.00	0.00	0.00	10750	3536	-	-		
100	10	18086	0	2	0	25	1800.00	1800.00	0.00	393.05	0.00	10750	3536	-	0.06	

Table 11: EVS-SOC-GLIN results for solving the static model versus B&C with $E_v^{\max\text{-lb}}$ and $E_v^{\max\text{-ex}}$ based on the original P_v^{\max} functions and $P_{\text{gridmax}} = 25n$.

n	Δt (min)	n_{seg}		n_{opt}		n_{feas}		Runtime (s)				n_{cuts}		%gap			
		Mean	StdDev	Static	B&C	Static	B&C	Static	B&C	Median	StdDev	Static	B&C	Median	StdDev	Static	B&C
$E_v^{\max\text{-lb}}$																	
5	1	155	12	5	30	29	30	1800.00	1800.00	690.82	636.49	3184	3153	0.02	0.06		
5	5	139	28	26	30	30	30	25.52	6.68	450.62	616.54	422	461	0.01	0.01		
5	10	119	30	29	30	30	30	1.27	1.62	10.37	329.09	153	154	0.01	0.01		
10	1	312	1	0	23	20	23	1800.00	1800.00	29.78	0.00	7298	2829	0.10	0.12		
10	5	279	29	19	30	30	30	183.39	770.59	445.94	815.87	1132	771	0.01	0.01		
10	10	242	30	29	30	30	30	17.87	11.88	163.75	437.28	452	223	0.01	0.01		
20	1	612	0	0	3	4	3	1800.00	1800.00	0.00	0.00	11938	2372	0.26	0.28		
20	5	553	14	6	30	30	30	1800.00	1800.00	608.45	637.22	2702	936	0.01	0.05		
20	10	475	29	22	30	30	30	60.59	201.06	422.28	755.21	967	359	0.01	0.01		
50	1	1544	0	0	0	0	0	1800.00	1800.00	0.00	0.00	22034	4220	-	-		
50	5	1393	2	1	29	29	30	1800.00	1800.00	160.23	280.55	6997	1257	0.08	0.11		
50	10	1192	20	5	30	30	30	902.21	1800.00	698.40	604.91	2575	653	0.01	0.03		
100	1	3095	0	0	0	0	0	1800.00	1800.00	0.00	0.00	29193	6236	-	-		
100	5	2796	0	0	14	14	7	1800.00	1800.00	0.00	0.00	11737	1494	0.12	0.18		
100	10	2399	6	0	30	30	30	1800.00	1800.00	482.70	0.00	5340	1077	0.03	0.06		
$E_v^{\max\text{-ex}}$																	
5	1	901	1	1	25	9	25	1800.00	1800.00	274.48	138.10	15258	9382	0.21	0.20		
5	5	901	26	17	30	30	30	448.47	761.59	644.73	831.42	2153	2330	0.01	0.01		
5	10	901	29	26	30	30	30	56.12	16.43	321.42	610.48	866	990	0.00	0.01		
10	1	1802	0	0	18	1	18	1800.00	1800.00	0.00	0.00	23328	9977	0.23	0.33		
10	5	1802	12	7	26	26	30	1800.00	1800.00	580.44	699.52	5220	3467	0.04	0.06		
10	10	1802	29	22	30	30	30	204.26	233.60	417.05	757.12	2063	1389	0.01	0.01		
20	1	3605	0	0	2	0	2	1800.00	1800.00	0.00	0.00	17970	9466	-	0.32		
20	5	3605	1	1	15	15	29	1800.00	1800.00	113.34	318.65	10784	4058	0.08	0.12		
20	10	3605	20	10	29	29	30	1097.26	1800.00	573.95	709.09	4647	2500	0.01	0.03		
50	1	9041	0	0	0	0	0	1800.00	1800.00	0.00	0.00	23986	9245	-	-		
50	5	9041	0	0	17	17	17	1800.00	1800.00	0.00	0.00	23708	5721	-	0.18		
50	10	9041	0	3	16	16	28	1800.00	1800.00	0.00	439.63	12160	4186	0.04	0.08		
100	1	18086	0	0	0	0	0	1800.00	1800.00	0.00	0.00	0	4697	-	-		
100	5	18086	0	0	0	0	0	1800.00	1800.00	0.00	0.00	25754	8585	-	-		
100	10	18086	0	0	19	19	19	1800.00	1800.00	0.00	0.00	19752	5121	-	0.09		

Table 12: EVS-SOC-GLIN results for solving the static model versus B&C with $E_v^{\max\text{-lb}}$ and $E_v^{\max\text{-ex}}$ based on the original P_v^{\max} functions and $P_{\text{gridmax}} = 40n$.

n	Δt (min)	n_{seg}		n_{opt}		n_{feas}		Runtime (s)				n_{cuts}		%gap		
		Mean		Static	B&C	Static	B&C	Static	B&C	Median	StdDev	Median	StdDev	Static	Median	B&C
$E_v^{\max\text{-lb}}$																
5	1	155	11	2	29	29	29	1800.00	1800.00	542.57	57.30	4476	2923	0.04	0.15	
5	5	139	28	24	30	30	30	31.04	55.93	513.40	715.78	619	492	0.01	0.01	
5	10	119	30	29	30	30	30	2.49	4.05	53.44	371.17	247	153	0.01	0.01	
10	1	311	0	0	20	20	20	1800.00	1800.00	0.00	0.00	8161	3130	0.21	0.17	
10	5	279	21	8	30	30	30	301.14	1800.00	745.75	677.68	1410	676	0.01	0.03	
10	10	242	28	26	30	30	30	27.80	36.06	450.92	660.00	456	201	0.01	0.01	
20	1	612	0	0	2	1	1	1800.00	1800.00	0.00	0.00	13361	2440	0.27	0.48	
20	5	553	5	0	30	30	30	1800.00	1800.00	365.20	0.00	2863	884	0.04	0.10	
20	10	475	28	19	30	30	30	69.51	571.16	479.77	745.04	1078	327	0.01	0.01	
50	1	1544	0	0	0	0	0	1800.00	1800.00	0.00	0.00	25908	3569	-	-	
50	5	1393	0	0	28	28	28	1800.00	1800.00	0.00	0.00	7110	1096	0.12	0.21	
50	10	1192	18	1	30	30	30	1097.80	1800.00	640.13	183.90	2748	520	0.01	0.05	
100	1	3095	0	0	0	0	0	1800.00	1800.00	0.00	0.00	29066	6072	-	-	
100	5	2796	0	0	7	2	2	1800.00	1800.00	0.00	0.00	11782	1239	0.22	0.21	
100	10	2399	1	0	29	30	30	1800.00	1800.00	121.93	0.00	5650	808	0.06	0.10	
$E_v^{\max\text{-ex}}$																
5	1	901	2	0	9	24	24	1800.00	1800.00	261.72	0.00	20190	9588	0.23	0.44	
5	5	901	25	9	30	30	30	582.18	1800.00	651.87	643.80	3180	2231	0.01	0.07	
5	10	901	30	23	30	30	30	80.12	34.07	160.32	753.56	1228	955	0.00	0.01	
10	1	1802	0	0	1	13	13	1800.00	1800.00	0.00	0.00	24450	8643	0.49	0.77	
10	5	1802	12	0	26	30	30	1800.00	1800.00	598.34	0.00	6026	3161	0.02	0.17	
10	10	1802	29	17	30	30	30	245.17	1147.26	375.49	837.79	2161	1553	0.01	0.01	
20	1	3605	0	0	0	0	0	1800.00	1800.00	0.00	0.00	17460	9716	-	-	
20	5	3605	0	0	15	29	29	1800.00	1800.00	0.00	0.00	13276	3457	0.14	0.22	
20	10	3605	19	3	29	30	30	1437.18	1800.00	550.74	447.72	5692	2190	0.01	0.08	
50	1	9041	0	0	0	0	0	1800.00	1800.00	0.00	0.00	12253	7961	-	-	
50	5	9041	0	0	0	11	11	1800.00	1800.00	0.00	0.00	27617	4805	-	0.21	
50	10	9041	0	0	14	27	27	1800.00	1800.00	0.00	0.00	13538	2670	0.10	0.12	
100	1	18083	0	0	0	0	0	-	1800.00	-	0.00	0	9122	-	-	
100	5	18086	0	0	0	0	0	1800.00	1800.00	0.00	0.00	31692	13113	-	-	
100	10	18086	0	0	0	11	11	1800.00	1800.00	0.00	0.00	23081	4035	-	0.14	

Table 13: EVS-SOC-GLIN results for solving the static model versus B&C with $E_u^{\max\text{-lb}}$ based on five-segment piecewise linear approximations of the original P_v^{\max} functions, $P_{\text{gridmax}} = 25n$.

n	Δt (min)	n_{seg}		n_{opt}		n_{feas}		Runtime (s)				n_{cuts}		% ϵ -gap	
		Mean	StdDev	Static	B&C	Static	B&C	Static	B&C	Median	StdDev	Median	StdDev	Static	B&C
$E_u^{\max\text{-lb}}$															
5	1	40	29	22	30	30	30	19.63	394.28	791.01	387	485	0.01	0.01	
5	5	46	30	30	30	30	30	1.98	5.97	263.17	88	102	0.01	0.01	
5	10	43	30	30	30	30	30	1.13	1.37	1.21	42	50	0.00	0.01	
10	1	80	27	13	30	30	30	1800.00	582.27	830.23	1162	639	0.01	0.02	
10	5	92	30	30	30	30	30	8.34	28.13	224.13	232	136	0.01	0.01	
10	10	87	30	30	30	30	30	1.49	1.78	8.36	118	62	0.01	0.01	
20	1	160	5	2	12	30	30	1800.00	193.77	407.09	2488	722	0.03	0.06	
20	5	185	30	25	30	30	30	54.58	199.06	659.96	516	192	0.01	0.01	
20	10	174	30	30	30	30	30	5.03	13.02	37.35	217	79	0.01	0.01	
50	1	398	0	0	0	12	1800.00	1800.00	0.00	0.00	5598	796	-	0.24	
50	5	459	28	10	30	30	30	640.74	516.17	754.54	1556	363	0.01	0.02	
50	10	433	30	29	30	30	30	37.23	54.09	379.05	624	160	0.01	0.01	
100	1	798	0	0	0	0	1800.00	1800.00	0.00	0.00	9312	1458	-	-	
100	5	921	12	3	30	30	30	1800.00	466.38	464.39	3237	568	0.01	0.06	
100	10	871	30	25	30	30	30	112.16	156.15	652.92	1360	259	0.01	0.01	

References

1. International Energy Agency. Global EV Outlook 2021, 2021.
2. Deilami, S.; Muyeen, S.M. An Insight into Practical Solutions for Electric Vehicle Charging in Smart Grid. *Energies* **2020**, *13*. doi:10.3390/en13071545.
3. Nicolson, M.L.; Fell, M.J.; Huebner, G.M. Consumer Demand for Time of Use Electricity Tariffs: A Systematized Review of the Empirical Evidence. *Renewable and Sustainable Energy Reviews* **2018**, *97*, 276–289.
4. Limmer, S. Dynamic Pricing for Electric Vehicle Charging—A Literature Review. *Energies* **2019**, *12*. doi:10.3390/en12183574.
5. Wang, Q.; Liu, X.; Du, J.; Kong, F. Smart Charging for Electric Vehicles: A Survey From the Algorithmic Perspective. *IEEE Communications Surveys Tutorials* **2016**, *18*, 1500–1517.
6. Fachrizal, R.; Shepero, M.; van der Meer, D.; Munkhammar, J.; Widén, J. Smart charging of electric vehicles considering photovoltaic power production and electricity consumption: A review. *eTransportation* **2020**, *4*.
7. Lopes, J.A.; Soares, F.; Almeida, P.; Moreira da Silva, M. Smart Charging Strategies for Electric Vehicles: Enhancing Grid Performance and Maximizing the Use of Variable Renewable Energy Resources. 24th International Battery, Hybrid and Fuel Cell Electric Vehicle Symposium & Exhibition 2009 (EVS24). The European Association for Electromobility (AVERE), 2009, Vol. 1, pp. 2680–2690.
8. Rotering, N.; Ilic, M. Optimal Charge Control of Plug-In Hybrid Electric Vehicles in Deregulated Electricity Markets. *IEEE Transactions on Power Systems* **2011**, *26*, 1021–1029.
9. Sortomme, E.; Hindi, M.M.; MacPherson, S.D.J.; Venkata, S.S. Coordinated Charging of Plug-In Hybrid Electric Vehicles to Minimize Distribution System Losses. *IEEE Transactions on Smart Grid* **2011**, *2*, 198–205.
10. Mehta, R.; Srinivasan, D.; Trivedi, A. Optimal charging scheduling of plug-in electric vehicles for maximizing penetration within a workplace car park. 2016 IEEE Congress on Evolutionary Computation (CEC). IEEE, 2016, pp. 3646–3653.
11. Goebel, C.; Jacobsen, H.A. Aggregator-Controlled EV Charging in Pay-as-Bid Reserve Markets With Strict Delivery Constraints. *IEEE Transactions on Power Systems* **2016**, *31*, 4447–4461.
12. Kontou, E.; Yin, Y.; Ge, Y.E. Cost-Effective and Ecofriendly Plug-In Hybrid Electric Vehicle Charging Management. *Transportation Research Record* **2017**, *2628*, 87–98.
13. Naharudinsyah, I.; Limmer, S. Optimal Charging of Electric Vehicles with Trading on the Intraday Electricity Market. *Energies* **2018**, *11*.
14. Huber, J.; Lohmann, K.; Schmidt, M.; Weinhardt, C. Carbon efficient smart charging using forecasts of marginal emission factors. *Journal of Cleaner Production* **2021**, *284*.
15. Fastned. Fastned – Supersnel laden langs de snelweg en in de stad: www.fastnedcharging.com, 2020.
16. Mies, J.J.; Helmus, J.R.; Van den Hoed, R. Estimating the Charging Profile of Individual Charge Sessions of Electric Vehicles in The Netherlands. *World Electric Vehicle Journal* **2018**, *9*. doi:10.3390/wevj9020017.
17. Frendo, O.; Graf, J.; Gaertner, N.; Stuckenschmidt, H. Data-driven smart charging for heterogeneous electric vehicle fleets. *Energy and AI* **2020**, *1*.
18. Korolko, N.; Sahinoglu, Z. Robust Optimization of EV Charging Schedules in Unregulated Electricity Markets. *IEEE Transactions on Smart Grid* **2017**, *8*, 149–157.
19. Schaden, B. Scheduling the Charging of Electric Vehicles with SOC-Dependent Maximum Charging Power. Master's thesis, TU Wien, 2021.
20. Sundström, O.; Binding, C. Optimization methods to plan the charging of electric vehicle fleets. Proceedings of the International Conference on Control, Communication and Power Engineering; , 2010; pp. 323–328.
21. Morstyn, T.; Crozier, C.; Deakin, M.; McCulloch, M.D. Conic Optimization for Electric Vehicle Station Smart Charging With Battery Voltage Constraints. *IEEE Transactions on Transportation Electrification* **2020**, *6*, 478–487.
22. Cao, Y.; Tang, S.; Li, C.; Zhang, P.; Tan, Y.; Zhang, Z.; Li, J. An Optimized EV Charging Model Considering TOU Price and SOC Curve. *IEEE Transactions on Smart Grid* **2012**, *3*, 388–393.
23. El-Bayeh, C.Z.; Mougharbel, I.; Saad, M.; Chandra, A.; Asber, D.; Lefebvre, S. Impact of Considering Variable Battery Power Profile of Electric Vehicles on the Distribution Network. 2018 4th International Conference on Renewable Energies for Developing Countries (REDEC). IEEE, 2018, pp. 1–8.
24. Han, J.; Park, J.; Lee, K. Optimal Scheduling for Electric Vehicle Charging under Variable Maximum Charging Power. *Energies* **2017**, *10*.
25. Bertsimas, D.; Tsitsiklis, J.N. *Introduction to linear optimisation*; Vol. 6, *Athena scientific optimization and computation series*, Athena Scientific, 1997.
26. Jekel, C.F.; Venter, G. *pwl: A Python Library for Fitting 1D Continuous Piecewise Linear Functions*, 2019.
27. Ishihara, T.; Limmer, S. Optimizing the Hyperparameters of a Mixed Integer Linear Programming Solver to Speed up Electric Vehicle Charging Control. Applications of Evolutionary Computation; Castillo, P.A.; Jiménez Laredo, J.L.; Fernández de Vega, F., Eds. Springer, 2020, Vol. 12104, *LNCS*, pp. 37–53.